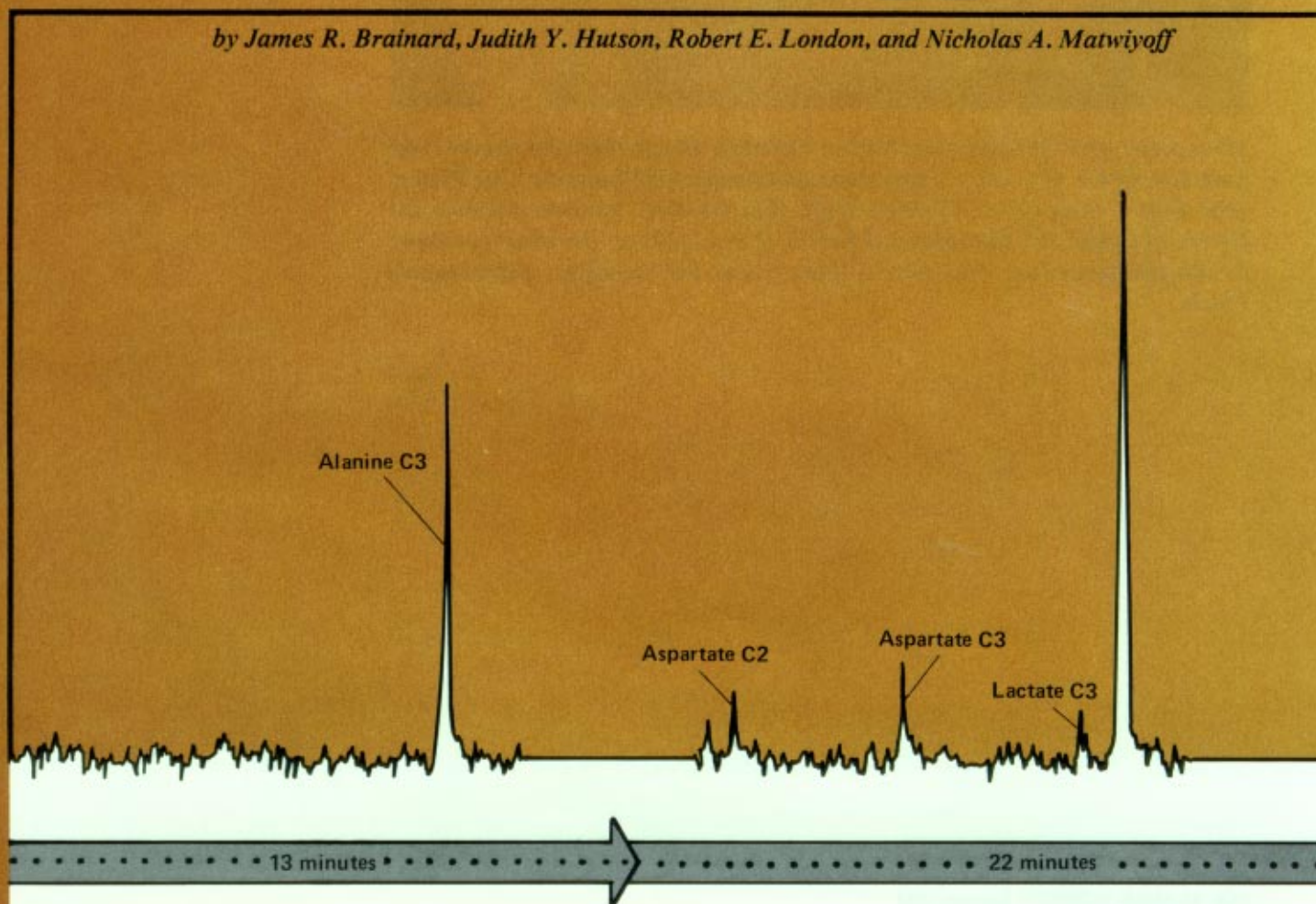


*What happens to your body when you drink alcohol? How does your metabolism change when your oxygen supply is reduced? How does one know that an organ is healthy enough to be used as a transplant? Why do some people persistently have low blood sugar? The only way to find out in detail is to watch*

# Metabolism

## *as it happens*

*by James R. Brainard, Judith Y. Hutson, Robert E. London, and Nicholas A. Matwiyoff*



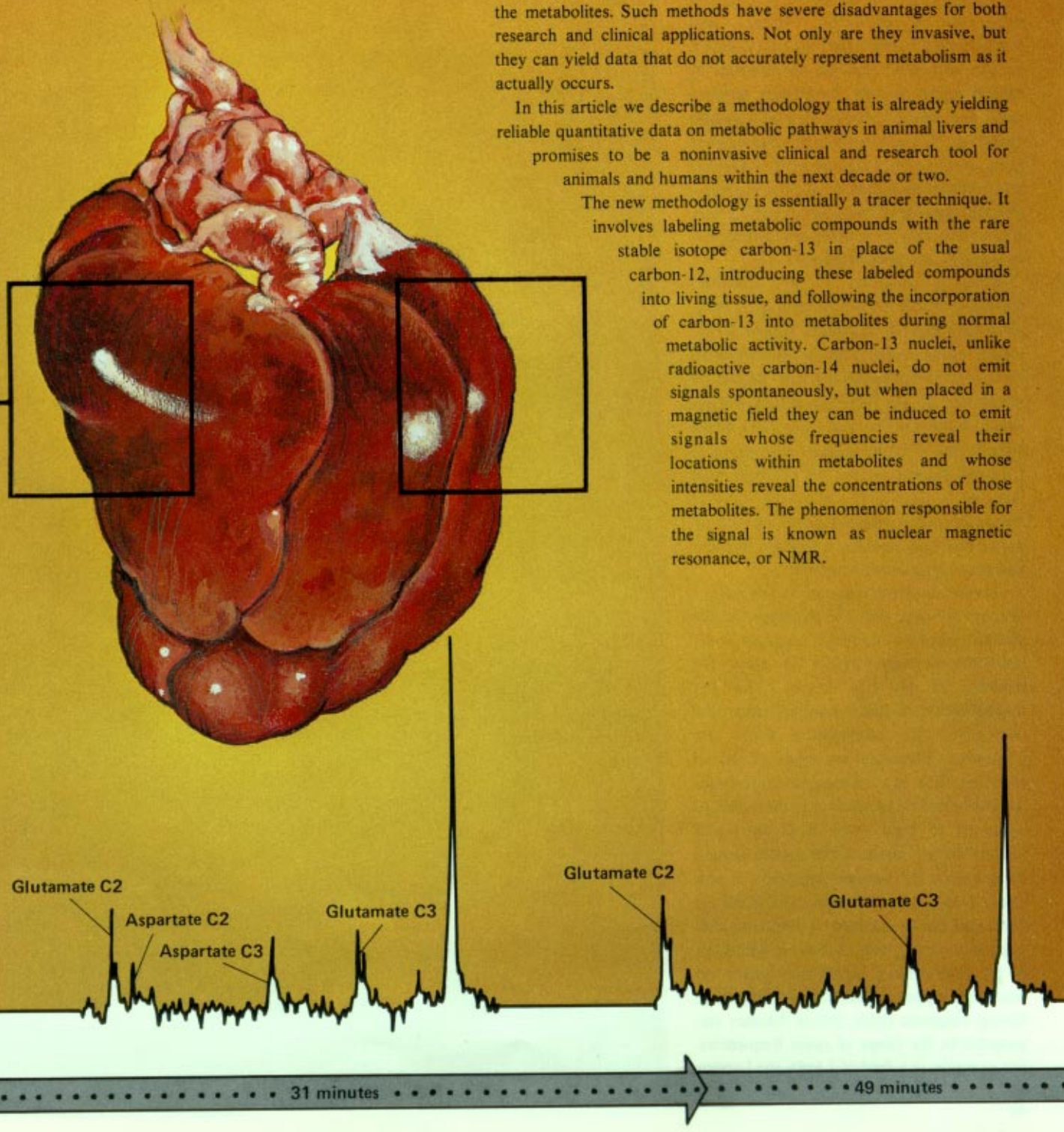
**T**he liver is primary among the organs responsible for regulating metabolism. It is the first organ to process nutrients coming from the intestine, and since these nutrients have a highly variable composition, the liver must continuously adjust its metabolic activities to maintain relatively constant concentrations of nutrients in the blood stream. This regulation is achieved by a very complex network of chemical

reactions with numerous checks and balances. Sometimes the network goes awry, and when it does, chronic disorders are the result. Abnormal metabolism of glucose, for example, accompanies diabetes, hypoglycemia, obesity, and glycogen storage diseases.

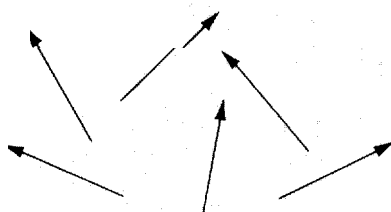
These diseases can best be diagnosed and treated—or prevented—if their molecular basis is understood. But until recently the only methods available to examine metabolic activity required removing body fluids or tissues, working up samples, and isolating the metabolites. Such methods have severe disadvantages for both research and clinical applications. Not only are they invasive, but they can yield data that do not accurately represent metabolism as it actually occurs.

In this article we describe a methodology that is already yielding reliable quantitative data on metabolic pathways in animal livers and promises to be a noninvasive clinical and research tool for animals and humans within the next decade or two.

The new methodology is essentially a tracer technique. It involves labeling metabolic compounds with the rare stable isotope carbon-13 in place of the usual carbon-12, introducing these labeled compounds into living tissue, and following the incorporation of carbon-13 into metabolites during normal metabolic activity. Carbon-13 nuclei, unlike radioactive carbon-14 nuclei, do not emit signals spontaneously, but when placed in a magnetic field they can be induced to emit signals whose frequencies reveal their locations within metabolites and whose intensities reveal the concentrations of those metabolites. The phenomenon responsible for the signal is known as nuclear magnetic resonance, or NMR.



(a) No Magnetic Field



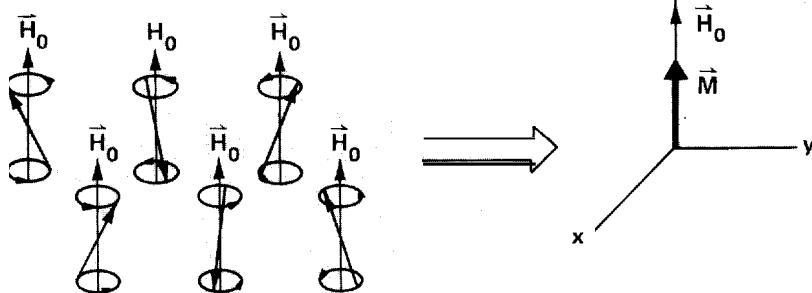
## Principles of NMR Spectroscopy

Nuclear magnetic resonance (Fig. 1) has been used by physicists, chemists, and biochemists for almost four decades to examine the properties and the environment of certain nuclei, namely those with nonzero spins and hence nonzero nuclear magnetic moments. All nuclei with odd mass number (and some nuclei with odd proton number and odd neutron number) have this property, and the nuclei most commonly used in NMR studies of biological systems are hydrogen-1, carbon-13, and phosphorus-31.

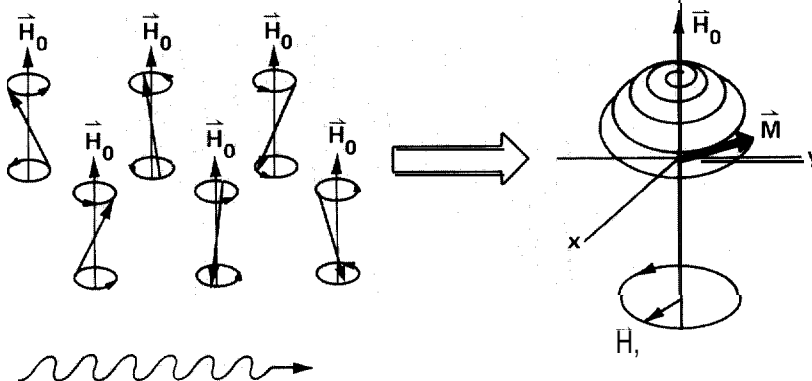
When a collection of (for example) carbon-13 nuclei are placed in a static magnetic field  $H_0$ , the individual magnetic moments, which usually point in random directions, tend to line up either almost parallel or antiparallel to  $H_0$ . (The two possible alignments reflect the fact that carbon-13 nuclei have a spin of  $\frac{1}{2}$ .) In addition, the magnetic moments precess around the magnetic field lines at a frequency, called the Larmor frequency, that is proportional to the product of carbon-13's nuclear magnetic moment and the magnetic field strength.

How do we detect these precessing nuclei? We use the fact that the alignment of the nuclear magnetic moments produces a net macroscopic magnetization  $M$  along the direction of  $H_0$  (the z-axis). This net magnetization is static, however, and does not give any information about the precession. Therefore we apply a second magnetic field  $H_1$ , rotating at the Larmor frequency and perpendicular to the z-axis, to cause  $M$  to bend away from the z-axis toward the x-y plane. As  $M$  rotates around the z-axis at the Larmor frequency, it produces a fluctuating magnetization in the x-y plane that can be detected by sensitive radio-frequency pickup coils. A Fourier transform of the time-varying signal then yields the resonance signal at the Larmor frequency. Strong magnetic fields induce Larmor frequencies in the range of radio frequencies. For example, in a field of 1 tesla, the Larmor

(b) Static Magnetic Field  $\vec{H}_0$  Along z Direction



(c) Second Magnetic Field  $\vec{H}_1$  in x-y Plane Oscillating at Frequency  $\omega$



(d) Signal Detected as  $M$  Rotates in x-y Plane at Frequency  $\omega$

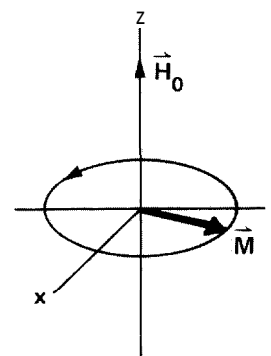


**Fig. 1. Carbon-13 nuclear magnetic resonance.**

(a) A carbon-13 nucleus has a spin of  $\frac{1}{2}$  and a nonzero nuclear magnetic moment  $\mu$ . The moments of a collection of carbon-13 nuclei are randomly oriented in the absence of an external magnetic field.

(b) In a static external magnetic field  $H_0$ , the moments become aligned almost parallel or antiparallel to  $H_0$  and precess around the field lines at a frequency  $\omega \propto \mu H_0$ . More moments point "up" (in the direction of  $H_0$ ) than "down" because the "up" state is lower in energy than the "down" state by an amount  $h\nu$ . Consequently, the sum of the moments yields a net macroscopic magnetization  $M$  in the direction of  $H_0$ . Since the moments do not precess in phase, they do not produce a net magnetization in the x-y plane.

(c) To measure  $\omega$ , one applies an oscillating magnetic field perpendicular to  $H_0$ . If the frequency of this field matches (is in resonance with) the Larmor frequency  $\omega$ , it induces transitions between the two states. The resulting net absorption of energy could serve as the resonance signal, but most modern spectrometers measure the effect of the oscillating magnetic field on  $M$ . The oscillating field may be decomposed into two rotating fields, one of which,  $H_1$ , rotates in the same direction as the processing nuclei. On a classical level we may say that  $H_1$  exerts a torque on  $M$  such that  $M$  spirals down toward the x-y plane. The result is a net magnetization in the x-y plane that fluctuates at the frequency  $\omega$ .

(d)  $H_1$  is often applied as a radio-frequency pulse whose intensity and duration insure that at the end of the pulse  $M$  is rotating in the x-y plane.

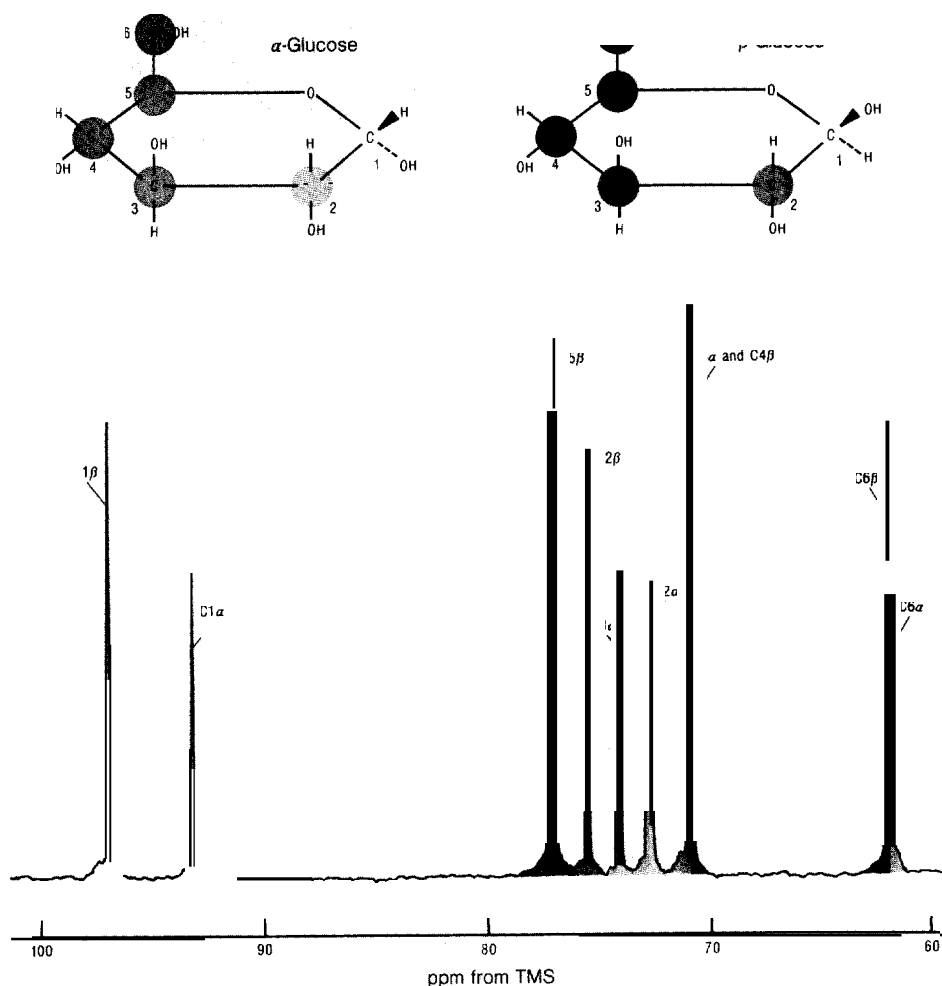


**Fig. 2. NMR spectrum of the naturally occurring carbon-13 nuclei in glucose.** All but two of the twelve different frequencies are clearly resolved in the spectrum shown here, which was obtained with a 2.3-tesla static magnetic field and a 25.2-megahertz rotating magnetic field. The resonance peaks are labeled and color-coded according to carbon position and anomeric form. The resonance frequencies are expressed as relative deviations (in ppm) from the resonance frequency of carbon-13 in the reference molecule tetramethylsilane, or TMS. This spectrum would have contained many more carbon-13 resonances had the protons of glucose been allowed to line up with the static magnetic field and produce magnetic fields that interact with the carbon-13 nuclei. These interactions are averaged—and a single resonance is obtained for each nonequivalent carbon location—by introducing a magnetic field oscillating at the Larmor frequency of the protons. The relative intensities of the resonances for the  $\alpha$  and  $\beta$  anomers are related to their relative abundances.

frequency of carbon-13 nuclei is 10.7 megahertz and that of protons is 42.6 megahertz. Note that since the magnetic moment varies from one isotope to another, different isotopes in the same magnetic field have different Larmor frequencies.

Chemically bound nuclei, as opposed to free nuclei, also exhibit nuclear magnetic resonance but resonate at slightly different frequencies depending upon their chemical environment. Consequently, identical nuclei

at nonequivalent locations within a molecule will give rise to separate resonance peaks. The ratio of the separation between the peaks to the frequency of any one peak is typically on the order of parts per million. These so-called chemical shifts in resonance frequency come about because the surrounding electrons tend to shield the nuclei from the applied magnetic field. Thus nuclei in electron-rich environments see a lower field and resonate at lower frequencies than do

nuclei in electron-poor environments.

An illustration of chemical shifts is given in Fig. 2, the NMR spectrum of the naturally occurring carbon-13 nuclei in D-glucose ( $C_6H_{12}O_6$ ). Since glucose contains six nonequivalent carbon atoms, one might predict that the spectrum would contain six distinct carbon-13 resonances. However, glucose exists in two anomeric forms,  $\alpha$  and  $\beta$ , characterized by different configurations of the hydroxyl group ( $-OH$ ) on carbon 1.

Consequently, its spectrum contains not six but twelve resonances corresponding to six carbons in two anomeric forms. The separation between the  $\alpha$  and  $\beta$  peaks of carbon 6, a location relatively distant from the anomeric carbon atom, is testimony to the ability of NMR spectroscopy to detect rather subtle structural features. In addition, proper selection of instrumental parameters makes it possible to determine the relative amounts of different substances directly from the relative intensities of the resonances. For example, from the relative intensities of the resonances of the  $\alpha$  and  $\beta$  anomers in Fig. 2, we can calculate that the  $\beta$  anomer predominates by a factor of 2,

For our experiments with  $^{13}\text{C}$ -labeled molecules, we use a pulsed NMR technique in which the applied radio-frequency pulse has a bandwidth that covers the spread in carbon-13 resonance frequencies. A Fourier transform of the time-varying signal induced by the pulse then yields the frequencies of all the carbon-13 resonances.

### Early NMR Studies of Metabolism *in Vivo*

About ten years ago one of us (Matwiyoff) began to explore the utility of applying carbon-13 labeling and NMR spectroscopy to monitor metabolic processes in living systems. The Laboratory was already involved in separating carbon-13 from carbon-12 and in finding methods to incorporate this isotope into organic molecules. Since carbon-13 is chemically identical to carbon-12,  $^{13}\text{C}$ -labeled molecules could be introduced into living systems without compromising their biochemical activity. Moreover, since carbon-13 is normally present in organic molecules at very low levels (1.1 percent), its introduction through labeling would greatly enhance the sensitivity of NMR tracer studies. Such studies require subjecting living systems to magnetic and radio-frequency fields, but these fields are essentially nondestructive.

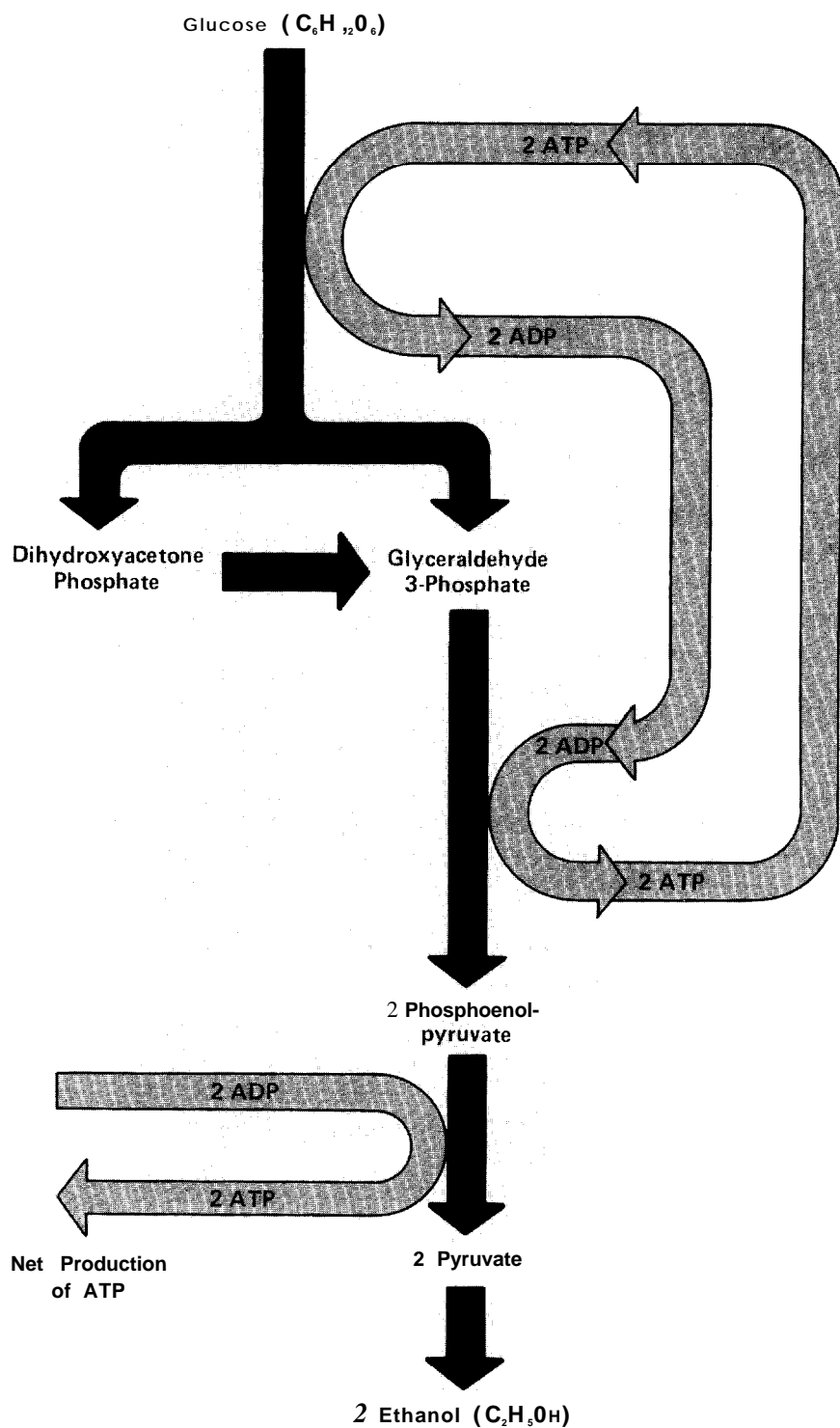


**Fig. 3. Glycolysis in yeast cells under anaerobic conditions. This pathway, which occurs in many types of cells, produces ATP by converting glucose to pyruvate. ATP provides the energy required for many cellular processes. The 6-carbon sugar glucose is first converted (in four steps) to two 3-carbon carbohydrates (glyceraldehyde 3-phosphate and dihydroxyacetone phosphate) with the consumption of two molecules of ATP. These ATP molecules are regenerated, however, as two molecules of phosphoenolpyruvate are formed from the 3-carbon carbohydrates. Subsequent hydrolysis of the phosphoenolpyruvate molecules to pyruvate is accompanied by the production of two molecules of ATP. Consequently, glycolysis yields a net production of ATP. In yeast cells under anaerobic conditions, the pyruvate is converted to ethanol.**

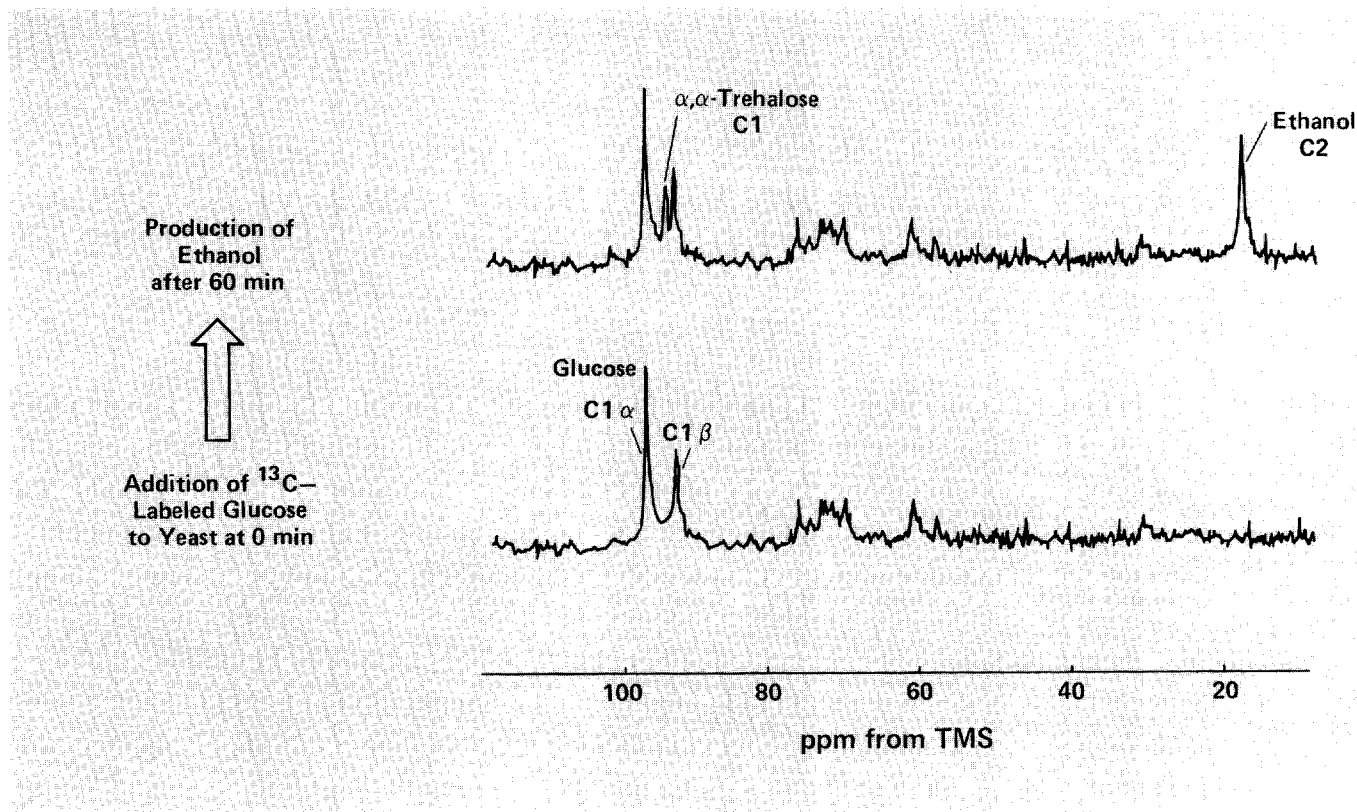


**Fig. 4.** Proton-decoupled carbon-13 NMR spectra of a suspension of yeast cells after addition of 5.5-millimolar [ $^{13}\text{C}$ ]glucose as a substrate for glycolysis. The spectrum taken immediately after addition of [ $^{13}\text{C}$ ]glucose shows resonances

only from the labeled carbon of glucose in its two anomeric forms. The spectrum taken after 60 minutes of metabolism shows, in addition, resonances from ethanol and  $\alpha,\alpha$ -trehalose, a storage form of glucose in yeast.

The first *in vivo* study of metabolism monitored the conversion of glucose to ethanol in yeast cells. Glucose, an energy-rich molecule, is broken down by living systems in a sequence of chemical reactions known as the glycolytic pathway (Fig. 3). The function of this sequence is to produce ATP (adenosine triphosphate), a molecule whose high chemical energy is used to drive many biochemical reactions.

Glucose labeled with carbon-13 (90 atomic percent) at carbon 1 ([ $^{13}\text{C}$ ]glucose) was added to a suspension of yeast cells, and the course of its conversion to ethanol was followed with NMR spectra (Fig. 4). The initial spectrum, obtained shortly after the addition of [ $^{13}\text{C}$ ]glucose, showed only two intense resonances, those from the  $\alpha$  and  $\beta$  configurations of the labeled carbon atom. After about an hour additional intense resonances appeared. One of these resonances was assigned to ethanol and the other to the disaccharide  $\alpha,\alpha$ -trehalose, which serves in yeast as a storage form of glucose. This experiment demonstrated that metabolism could be studied noninvasively and in real time within living organisms. Furthermore, it showed that the yeast cells converted a

portion of the glucose to ethanol to meet their immediate energy requirements and converted another portion into a storage form of carbohydrate.

From our early studies of metabolism in yeast and related studies of the structure of abnormal hemoglobin molecules in intact red blood cells, we were convinced that labeled metabolizes and NMR spectroscopy could be used with minimal invasiveness to study biochemical reactions as they occur *in vivo* under normal and pathological conditions. There has been slow but sustained progress toward this end in a number of laboratories, largely paralleling developments in NMR instrumentation. In this article we will emphasize the experimental strategies and information content of this methodology, using examples from ongoing research at Los Alamos.

#### Why Study Gluconeogenesis in the Liver?

In 1981 we acquired a high-field NMR spectrometer with a wide-bore magnet that allowed us to make the transition from the study of cells to the study of perfused

organs, that is, organs removed from the body but kept viable by circulation of an oxygenated blood-like medium through the organ. The study of perfused organs is a necessary next step toward applying the NMR technique to live animals. Although experiments on perfused organs preclude investigating relationships between different organs, they do allow us to change the composition or flow rate of the perfusion medium at will and thereby to study a wide variety of alterations in metabolism.

We chose to study the liver because of its central role in mammalian metabolism, and the primary question we addressed was whether carbon-13 NMR spectra could be used to detect changes in metabolism when the oxidation-reduction state or oxygen supply to the liver was changed. Correspondingly, could carbon-13 NMR metabolic profiles be used to predict the oxidation-reduction state and oxygen supply? We focused on one particular metabolic process, namely gluconeogenesis, or resynthesis of glucose. This process was chosen for several reasons. First, it has been well studied by classical methods, and the available data would provide a good check of our develop-

ing methodology. Second, the synthesized glucose accumulates in the liver and could therefore be easily detected by carbon-13 NMR. Finally, gluconeogenesis acts in competition with, parallel to, or synergistically with other metabolic pathways for the use of glucose and products of glucose metabolism. The other pathways include synthesis of glycogen, of fatty acids and other lipids, and of amino acids and glycoproteins. Thus a detailed understanding of gluconeogenesis under normal and abnormal oxidation-reduction states or oxygen supplies might provide insight into the regulation of many metabolic processes.

The body normally stores only enough glucose to provide fuel to the brain for twelve hours, and therefore the liver's unique ability to resynthesize glucose is extremely important for maintaining energy homeostasis. The glucose metabolized by the body supplies the precursors for gluconeogenesis. For example, muscle and brain cells oxidize glucose to pyruvate and lactate. Frequently, the pyruvate combines with an amino group ( $-\text{NH}_2$ ) to form the amino acid L-alanine, which is delivered by the blood stream to the liver where it is converted to glucose through gluconeogenesis.

This gluconeogenesis from alanine was the subject of our study. Figure 5 depicts its basic features and its relationship to oxygen supply. The figure shows the two components of the liver cell that participate in gluconeogenesis: the cytosol, or soluble portion of the cell, and the mitochondria, structures about the size of a bacterium surrounded by a double membrane. (The mitochondria use most of the oxygen supplied to the cell and are the sites of the principal energy-yielding reactions.)

The first step of gluconeogenesis takes place in the cytosol. There alanine, a 3-carbon amino acid, loses its amino group. (How the liver disposes of this amino group is an important question and will be considered later.) Alanine's 3-carbon skeleton then enters the mitochondria and undergoes

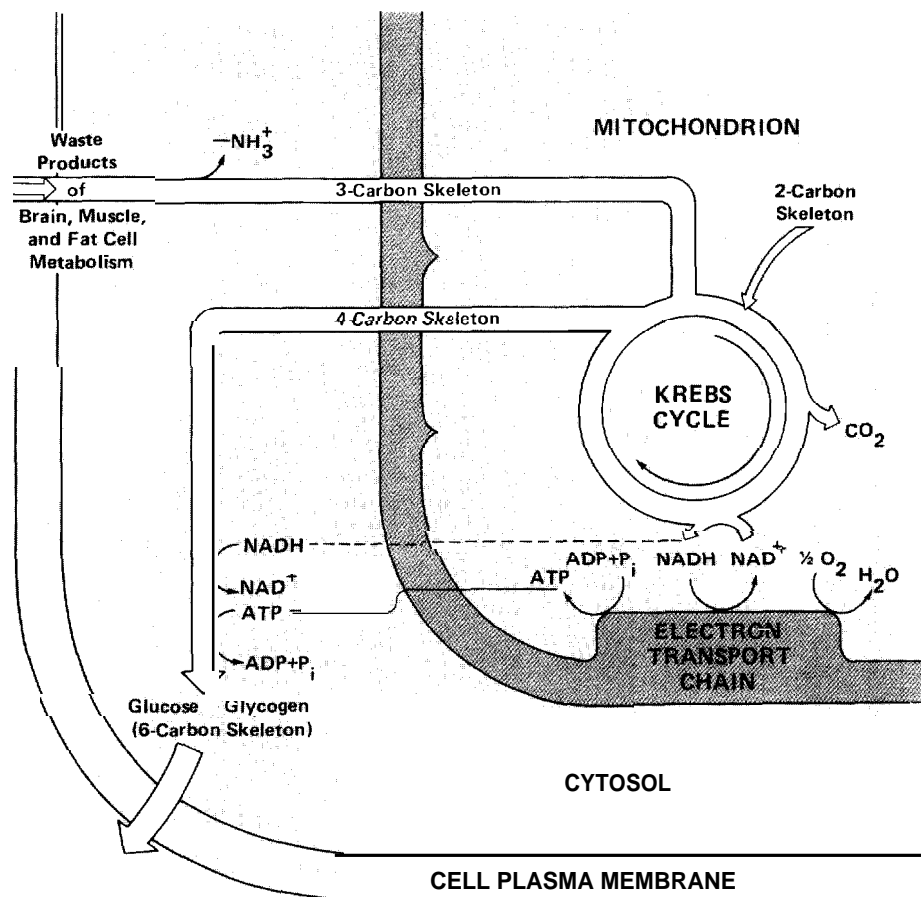


**Fig. 5. Gluconeogenesis, oxygen supply, and the Krebs cycle.** The white pathway traces gluconeogenesis: waste products of metabolism in muscle, brain, and fat cells enter the liver cell and glucose exits. This synthesis of glucose requires ATP and the reducing agent NADH. ATP is supplied by the electron transport chain in the mitochondrial membrane through a complex set of reactions that reduce oxygen. These reactions also regenerate the oxidizing agent  $\text{NAD}^+$ , which in turn is used in reactions in the Krebs cycle that yield NADH. Proper functioning of the electron transport chain depends on an adequate oxygen supply. The 4-carbon skeleton for gluconeogenesis is supplied by intermediates of the Krebs cycle. This cyclic sequence of enzymatic reactions in aerobic organisms serves primarily to convert chemical energy from carbohydrates, fatty acids, and amino acids into reduced pyridine nucleotides such as NADH, which are then used to produce ATP. Intermediates of the Krebs cycle form the building blocks for a variety of anabolic processes in addition to gluconeogenesis, and one of these intermediates, malate, transports reducing equivalents of NADH across the mitochondrial membrane. Such a mechanism is required since this membrane is impermeable to NADH itself.

one of two reactions (shown in Fig. 6). Products of these reactions enter the Krebs cycle and a 4-carbon skeleton emerges from the mitochondria. Two 4-carbon skeletons are then used in the cytosol to form glucose.

Although gluconeogenesis does not involve oxygen directly, it does require ATP and NADH (reduced nicotinamide adenine dinucleotide). The supply of these two substances depends on the supply of oxygen

to the electron transport chain in the mitochondrial membrane (see Fig. 5). NADH, a reducing agent, is produced from the oxidizing agent  $\text{NAD}^+$  by the Krebs cycle, and  $\text{NAD}^+$  is regenerated by the electron transport chain. Note that ATP can cross the mitochondrial membrane directly, but NADH cannot. Instead the reducing equivalents of NADH are transported to the cytosol indirectly by "shuttle" mechanisms



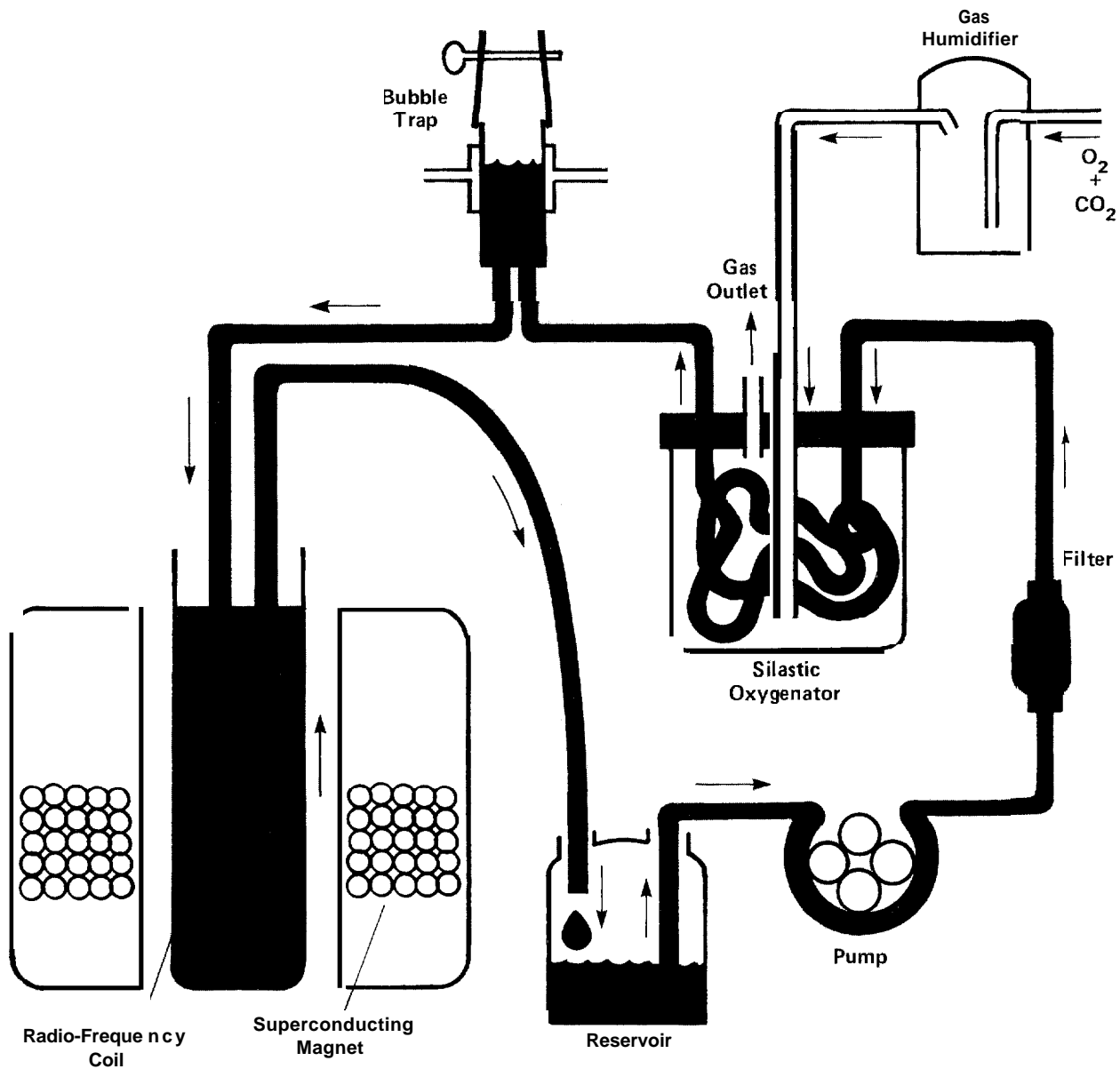
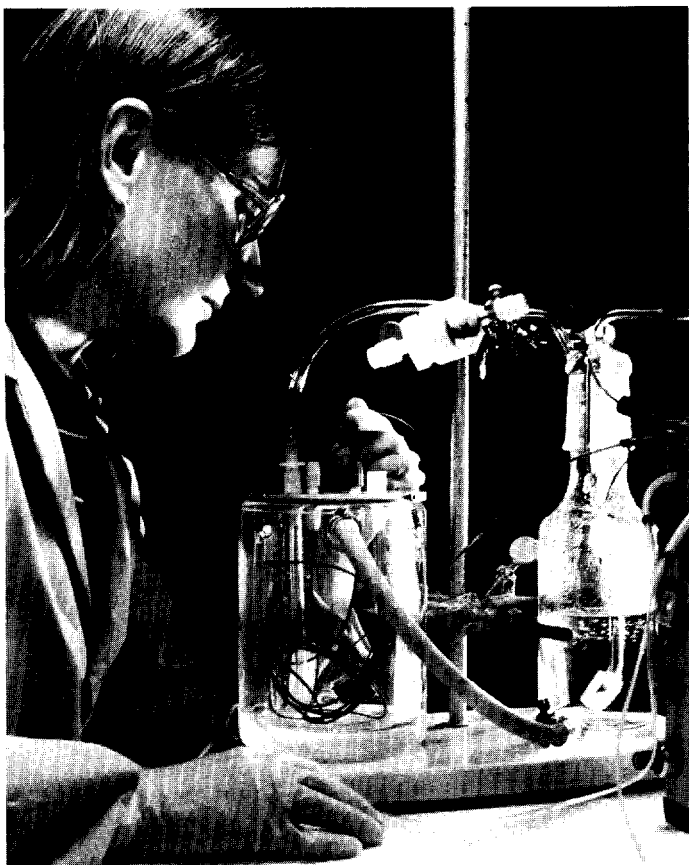


*Fig. 7. Apparatus for carbon-13 NMR spectroscopy on perfused Syrian hamster livers. The hamster is anesthetized, and a cannula is sutured into the portal vein of the liver. The liver, still in the hamster, is then supplied with oxygen and nutrients by the flow of perfusate into the vein. The liver is then*

*surgically removed from the animal and placed in a cylindrical sample tube, which is positioned in the bore of a 7.0-tesla superconducting magnet. The perfusate (a buffered saline solution containing 7 percent hemoglobin for increased oxygen-carrying ability) is recycled during the experiment.*



such as the malate shuttle shown in Fig. 6, a more detailed picture of gluconeogenesis. Figure 6 also shows that gluconeogenesis from alanine is coupled to the urea cycle (since the cell must dispose of amino groups) and as we shall see, to fatty acid degradation. Variations in the functioning of gluconeogenesis may thus provide a marker for a wide variety of metabolic disorders.

What happens to gluconeogenesis when the oxygen supply is reduced? For drastic decreases we know that the rate of gluconeogenesis is suppressed. But with carbon-13 NMR as a diagnostic tool, we can also detect subtle changes in metabolism caused by subtle changes in oxygen supply or in the oxidation-reduction state of the liver as defined by the NADH/NAD<sup>+</sup> ratio.

There is much clinical interest in under-

standing the regulatory effects of NADH/NAD<sup>+</sup> ratios because elevated NADH/NAD<sup>+</sup> ratios seem to be associated with fatty and cirrhotic livers. Elevated ratios can occur through the intake of alcohol or as a consequence of inadequate oxygen supply. If carbon-13 NMR studies of gluconeogenesis could enable us to assess the oxidation-reduction state of the liver under normal and stressful conditions, such as those induced by a dose of alcohol, we would be able to help identify those individuals at risk even in "social" drinking.

#### The Baseline Study of Gluconeogenesis

Before attempting to understand the regulation of gluconeogenesis by NADH/NAD<sup>+</sup>

ratios and to identify signs of disorder, we needed to monitor and understand in detail how gluconeogenesis proceeds under normal conditions. This in itself is a surprisingly intricate story that illustrates well the power of the carbon-13 NMR technique. We chose to study the liver from a small animal, the Syrian hamster, since it would easily fit into the 3-inch-bore magnet of our NMR spectrometer. Figure 7 is a diagram of the perfusion apparatus used to keep the liver viable and metabolically active after it has been surgically removed. The hamster was starved for 24 hours before the experiment to activate the enzymes involved in gluconeogenesis.

We monitored gluconeogenesis in the perfused liver with NMR spectra taken before and after addition of L-[3-<sup>13</sup>C] alanine

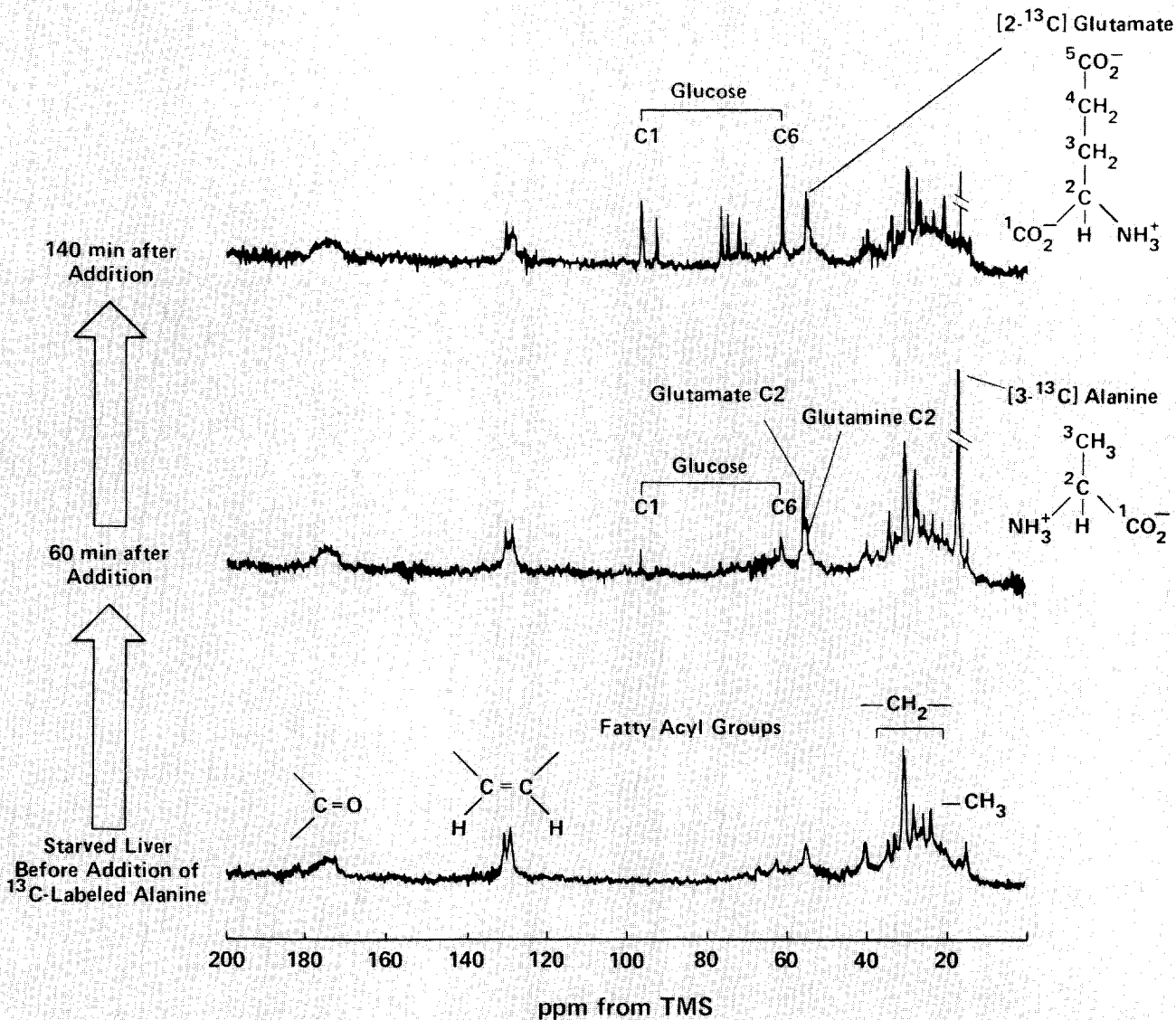


**Fig. 8. Carbon-13 NMR spectra from a perfused Syrian hamster liver performing gluconeogenesis from [3-<sup>13</sup>C]-alanine. The background spectrum, taken before addition of labeled alanine to the perfusate, shows resonances from lipids in the liver containing naturally occurring carbon-13. The**

**spectrum taken 60 minutes after addition of labeled alanine shows resonances from the amino acids glutamate and glutamine and from carbons 1 and 6 of glucose. By 140 minutes all carbon positions in glucose produce detectable resonances.**

to the perfusate (Fig. 8). The background spectrum, measured before addition of the labeled alanine, contains resonance peaks from the naturally occurring carbon-13 in lipids in the liver. The spectrum taken 60 minutes after addition of alanine contains a very intense resonance from the labeled carbon atom of alanine as well as less intense resonances from products of alanine metabolism in the liver. The most prominent products we detect are glutamate (which is

formed as alanine transfers its amino group to α-ketoglutarate) and glutamine (which is formed subsequently from glutamate). These amino acids provide a temporary sink for the amino group brought in by alanine. Glucose is also being produced but only in small quantities. After 140 minutes of perfusion, gluconeogenesis is in full swing and resonances from all carbon positions in glucose are detectable.

Since the background spectrum of the

liver might obscure resonances from metabolites that have acquired carbon-13 labels during the experiment, we subtract the background spectrum and examine the resulting "difference" spectra (Fig. 9). In these spectra we can identify resonances from carbons 2 and 3 of glutamate and glutamine, but a resonance from carbon 4 of glutamate is conspicuously absent.

The specific positions of the carbon-13 label in glutamate are extremely informative

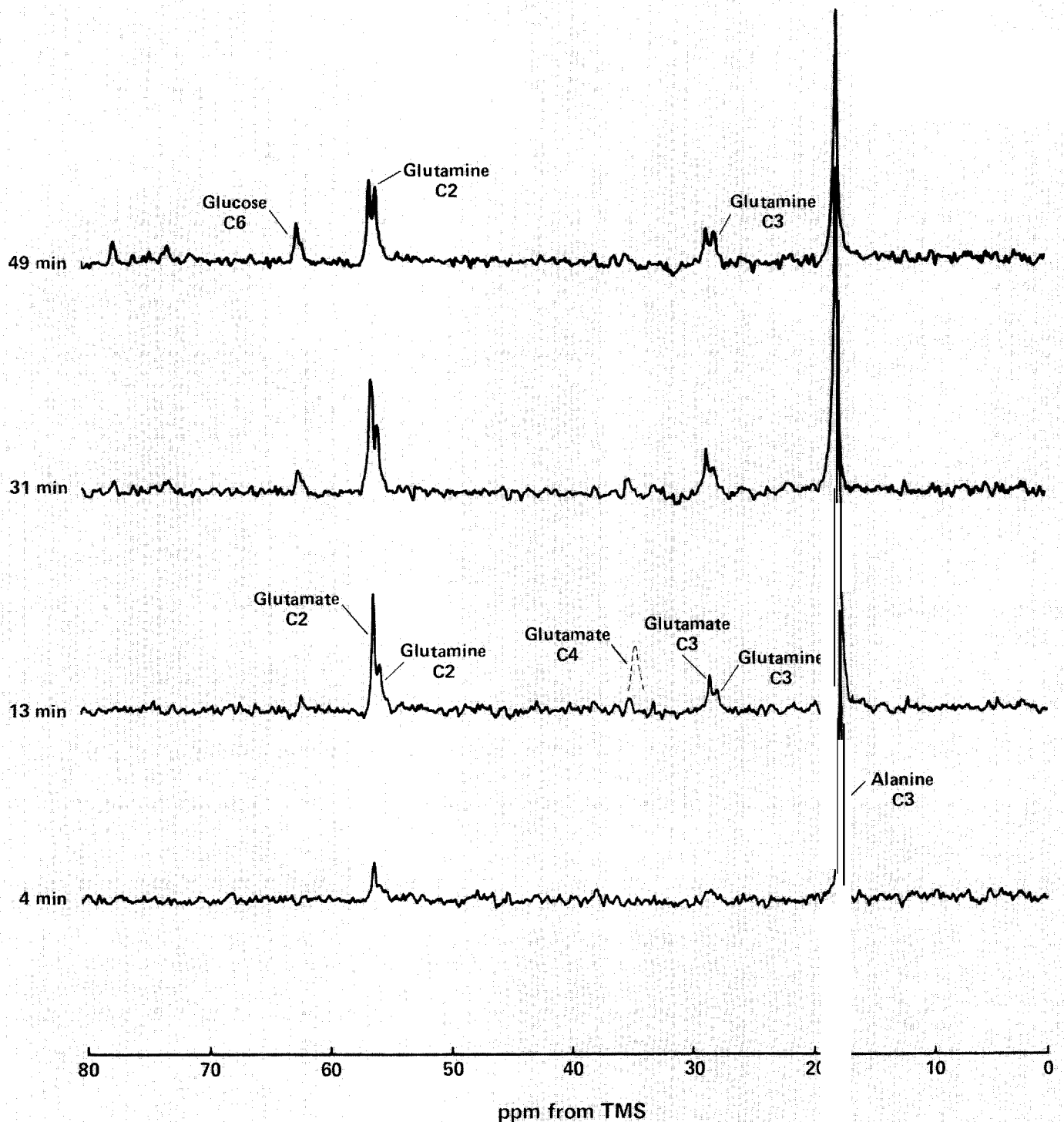
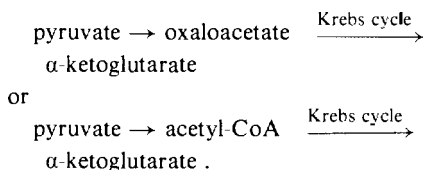


Fig. 9. Carbon-13 difference spectra of perfused Syrian hamster liver during the first hour of gluconeogenesis from 8-millimolar  $[3-^{13}\text{C}]$ alanine. These spectra are obtained by subtracting the background spectrum from each measured spectrum. The dashed peak occupies the position of the

nonexistent resonance from carbon 4 of glutamate. The presence of resonances from carbons 2 and 3 of glutamate and the absence of a resonance from carbon 4 show that label from alanine enters the Krebs cycle through oxaloacetate rather than acetyl-CoA (see Fig. 10).

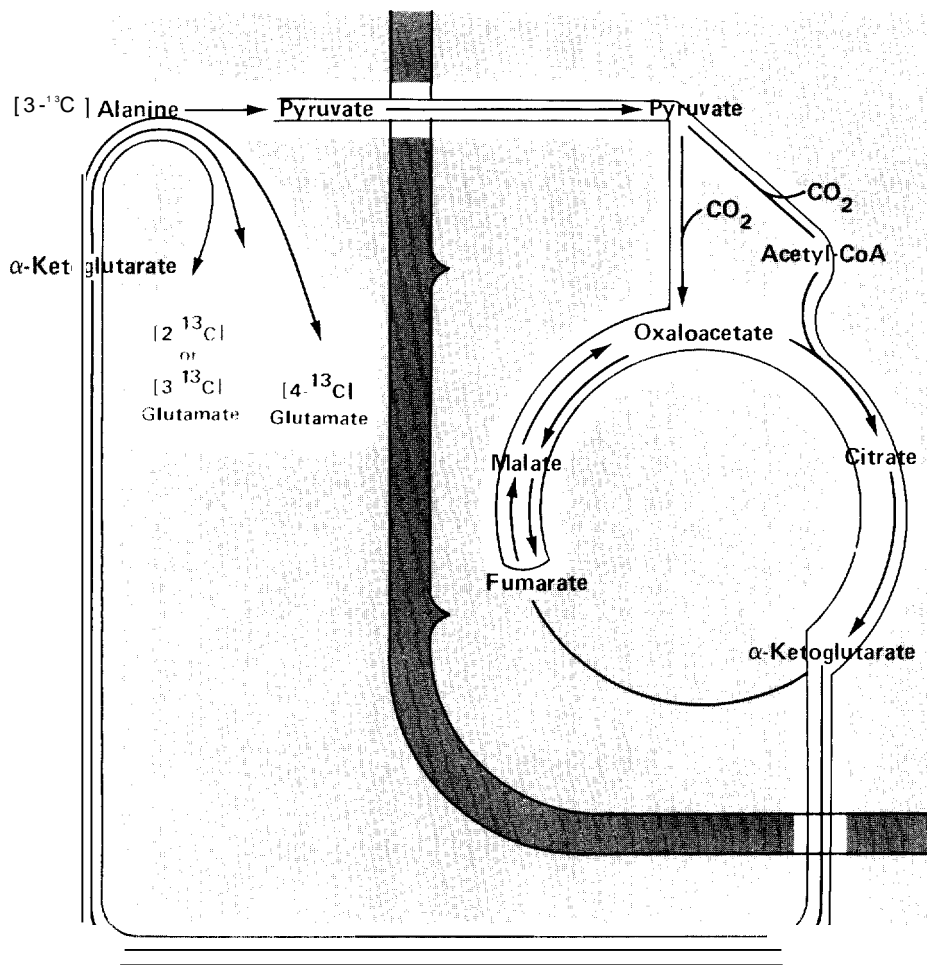
because they enable us to pinpoint the pathway by which glutamate was formed. To do this we use detailed information about the possible pathways to glutamate and the stereochemistry of the reactions involved (Fig. 10). This information has been accumulated from investigations with radio-labeled metabolites.

Figure 10 shows that glutamate acquires its carbon-13 label from  $\alpha$ -ketoglutarate made in the Krebs cycle. The figure also shows that  $\alpha$ -ketoglutarate can acquire its label in two ways depending upon how it is formed from the labeled pyruvate derived from  $[3-^{13}\text{C}]$ alanine:



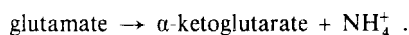
The pyruvate that enters the Krebs cycle as oxaloacetate will yield a mixture of  $[2-^{13}\text{C}]$ glutamate and  $[3-^{13}\text{C}]$ glutamate because of the equilibria among oxaloacetate, malate, and the symmetric Krebs cycle intermediate fumarate, which "scrambles" the label between carbons 2 and 3. On the other hand, the pyruvate entering the Krebs cycle as acetyl-CoA will yield only  $[4-^{13}\text{C}]$ glutamate. Since the spectra of Fig. 9 exhibited glutamate resonances only from carbons 2 and 3, we conclude that essentially all the alanine enters the Krebs cycle as oxaloacetate and that acetyl-CoA (which is required for Krebs-cycle activity) is derived, not from alanine, but from oxidation of lipids stored in the liver.

Before leaving the discussion of glutamate, we note another point of interest in the spectra of Fig. 9: after 60 minutes the glutamate resonances decrease rapidly in intensity but the glutamine resonances continue to increase. These two trends are not unrelated. Excess production of glutamate is disadvantageous to liver metabolism because it removes a key intermediate,  $\alpha$ -keto-



**Fig. 10.** Possible pathways for synthesis of glutamate during gluconeogenesis from  $[3-^{13}\text{C}]$ alanine and the stereochemistry of the reactions involved. Label from alanine may enter the pool of Krebs cycle intermediates through a pathway involving conversion of pyruvate to acetyl-CoA, which yields  $[4-^{13}\text{C}]$ glutamate, or through a pathway involving conversion of pyruvate to oxaloacetate, which yields a mixture of  $[2-^{13}\text{C}]$ glutamate and  $[3-^{13}\text{C}]$ glutamate. This "scrambling" of the label between carbons 2 and 3 (indicated in the figure by blue spotlights on each of the two possible carbon positions) is due to the reaction converting malate to the symmetric Krebs cycle intermediate fumarate. Since carbon-13 NMR spectra taken during gluconeogenesis by the liver from  $[3-^{13}\text{C}]$ alanine (Fig. 9) do not reveal a resonance from carbon 4 of glutamate, we conclude that essentially all of the label from alanine enters the pool of Krebs cycle intermediates as oxaloacetate rather than acetyl-CoA.

glutamate, from the Krebs cycle and thus reduces the ATP-generating capability of the mitochondria. Therefore the liver regenerates  $\alpha$ -ketoglutarate through the reaction

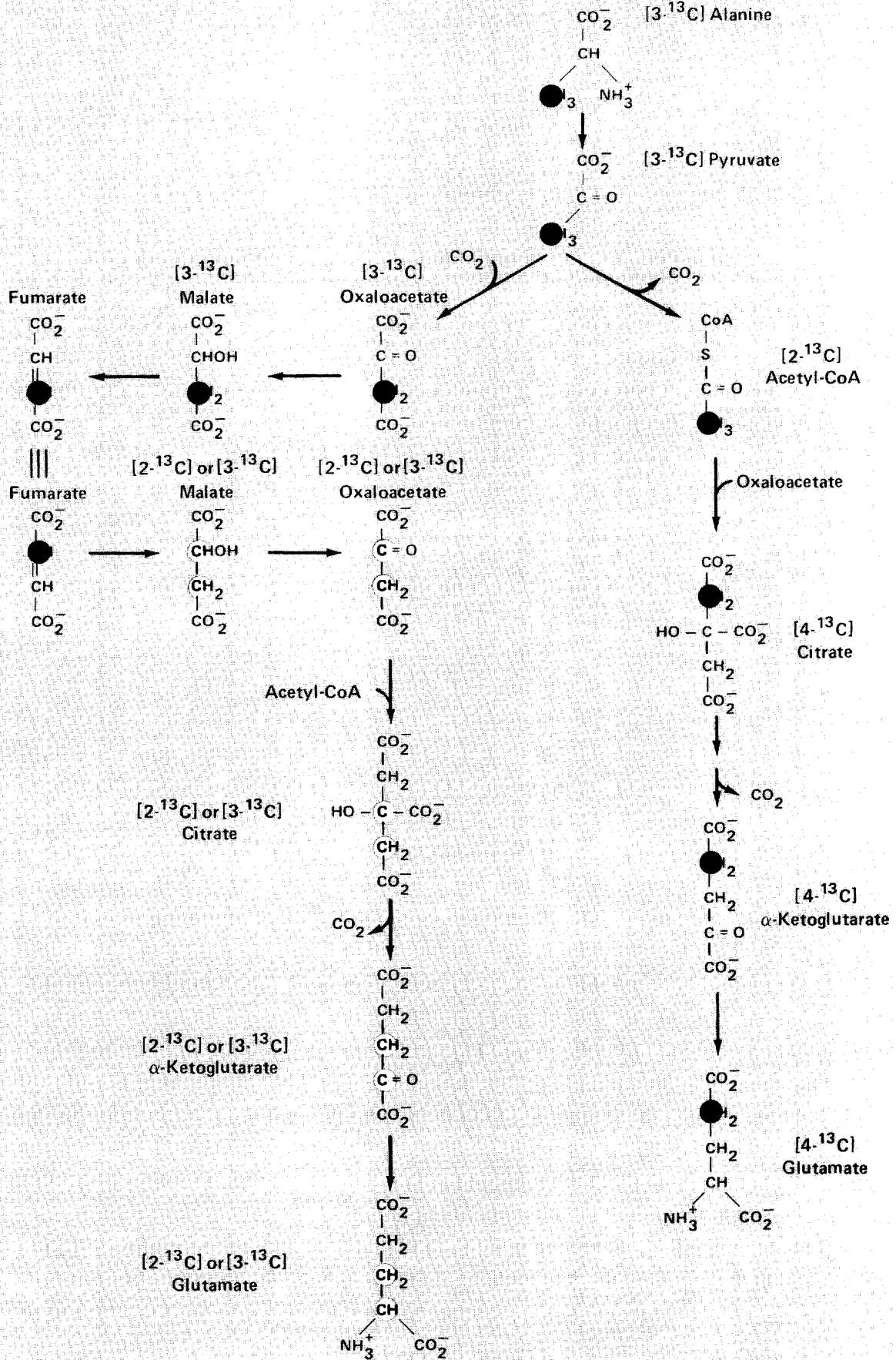


This use of glutamate explains the observed decrease in intensity of the glutamate resonances. Since the ammonium ion ( $\text{NH}_4^+$ ) produced in this reaction is very toxic to the liver, its concentration is in turn controlled

by the reaction



which explains the increasing intensity of the glutamine resonances. The formation of glutamine provides a sink for  $\text{NH}_4^+$  during gluconeogenesis from alanine. The formation of urea, another nitrogen-containing metabolite, also contributes substantially to maintaining proper  $\text{NH}_4^+$  concentrations and will be discussed later.



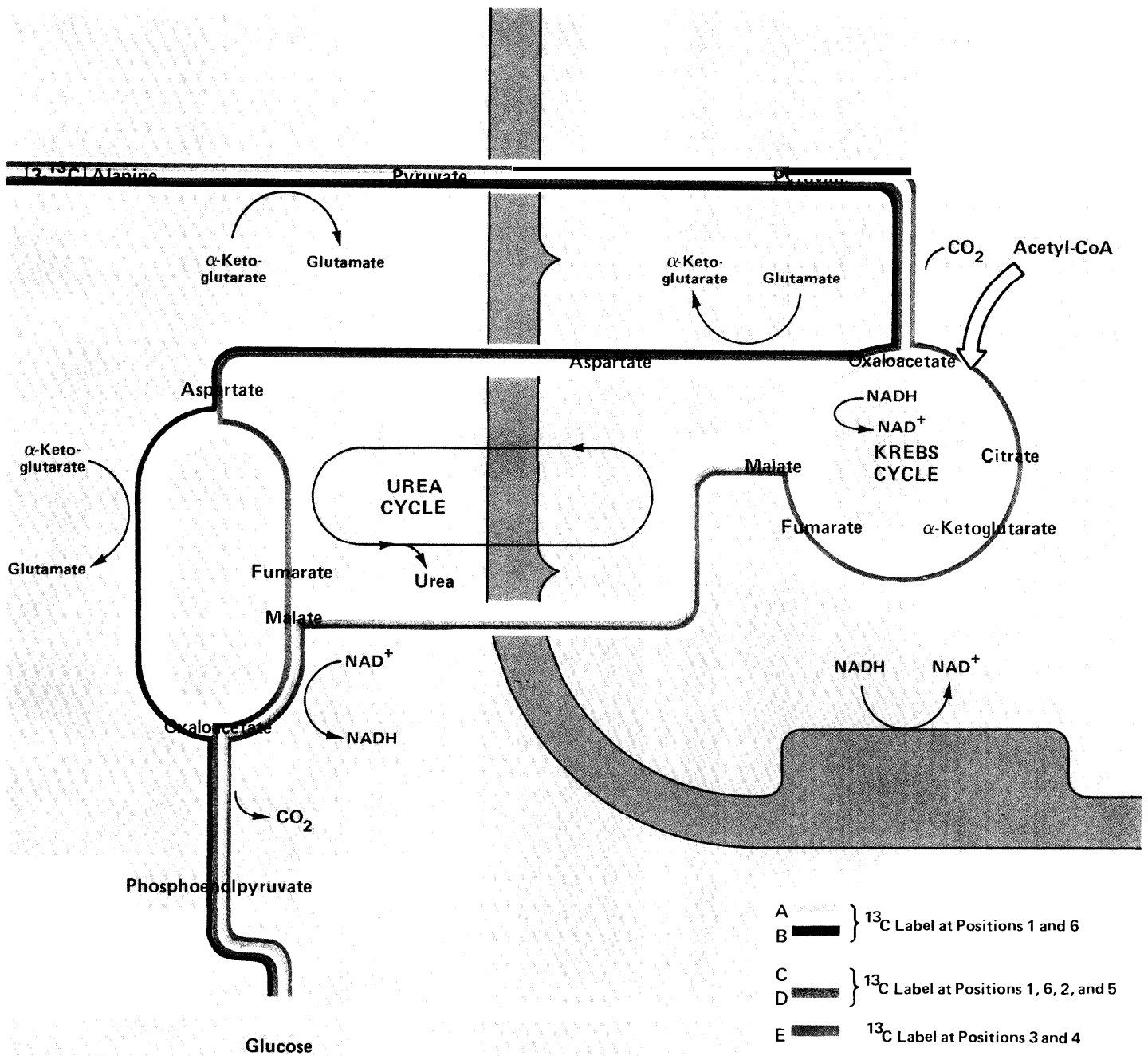
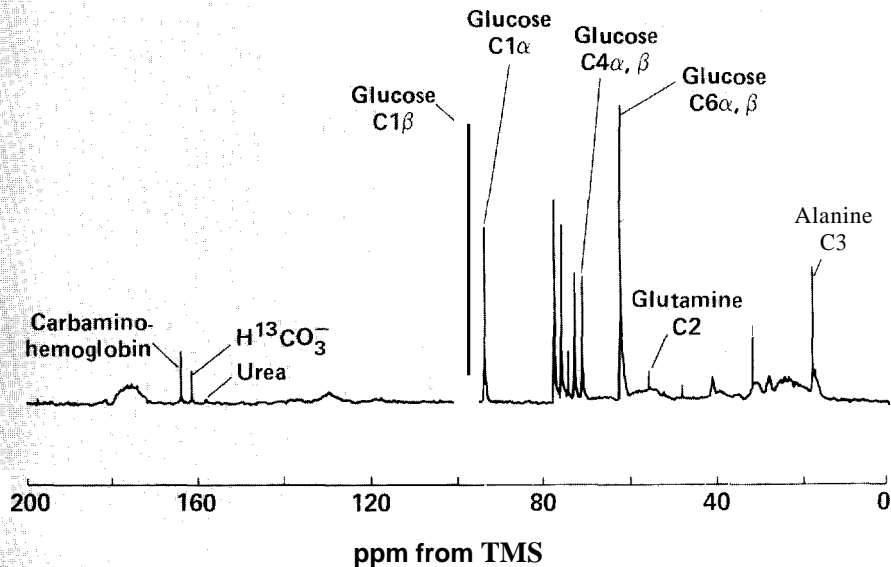


Fig. 11. Pathways for synthesis of glucose during gluconeogenesis from  $[3-^{13}\text{C}]$ alanine. Pathway A (reduction of oxaloacetate to malate in the mitochondria and the reverse of this reaction in the cytosol) and pathway B (conversion of oxaloacetate to aspartate in the mitochondria and the reverse of this reaction in the cytosol) yield glucose labeled at positions 1 and 6. Pathway C is identical to pathway A except for involvement of fumarate, which scrambles the label. Pathway D involves conversion of oxaloacetate to aspartate in the mitochondria (as in pathway B), but then, instead of being

directly converted back to oxaloacetate, aspartate participates in the urea cycle. Consequently, the label is scrambled through fumarate. Pathways C and D both yield glucose labeled at positions 1, 2, 5, and 6. Pathway E, in which oxaloacetate is converted to citrate and continues around the Krebs cycle, yields glucose labeled at positions 3 and 4. The fractions of glucose produced by the combination of pathways A and B, the combination of pathways C and D, and pathway E can be determined from the relative intensities of the resonances assigned to the various carbon positions in glucose.



**Fig. 12.** Proton-decoupled carbon-13 NMR spectrum of the medium used to perfuse the liver during gluconeogenesis from  $[3\text{-}^{13}\text{C}]$ alanine. This perfusate spectrum exhibits better resolution of the glucose resonances than does the liver spectrum (Fig. 9) and is therefore used to determine the relative fluxes of carbon-13 through the pathways of gluconeogenesis. This spectrum also shows resonances from labeled glutamine, bicarbonate, carbaminohemoglobin, and urea. The last three substances are formed from carbon dioxide, some of which acquires carbon-13 through oxidation of the  $^{13}\text{C}$ -labeled alanine and some through oxidation of fatty acids containing naturally occurring carbon-13.

from the relative intensities of the glucose resonances, although for a pair of degenerate pathways (such as A and B in Fig. 11), we obtain only a combined relative flux.

The relative flux of label through the pathways could be determined from the liver spectrum itself (Fig. 8), but the accuracy would be compromised by the poor resolution of the closely spaced resonances. Since some glucose diffuses out of the liver and into the perfusate, we used instead a spectrum from the isolated perfusate (Fig. 12), which exhibits better resolution because the perfusate is considerably more homogeneous. This spectrum also shows the presence of other labeled metabolites, such as bicarbonate ion ( $\text{HCO}_3^-$ ) and urea, that readily diffuse out of the liver.

Table I lists the values calculated from the perfusate spectrum for the relative fluxes of label through the pathways of Fig. 11 when the liver is well oxygenated and  $[3\text{-}^{13}\text{C}]$ alanine is the sole substrate. The combination of pathway A (the conversion of oxaloacetate through malate to glucose) and pathway B (the conversion of oxaloacetate to aspartate in the mitochondria and the reversal of this reaction in the cytosol) yields about 13 percent of the observed glucose. The combination of pathway C (fumarate scrambling of the malate pathway) and pathway D (through aspartate and its participation in the urea cycle) yields about 64 percent. About 21 percent of the glucose is derived from conversion of oxaloacetate through citrate and malate to glucose (pathway E).

Note that the flux through pathway E draws on the total mitochondrial pool of oxaloacetate and is therefore a measure of Krebs cycle activity. However, we measure the *relative* flux through pathway E, that is, the flux through pathway E divided by the total flux through all the gluconeogenesis pathways. Thus we can determine whether Krebs cycle activity is increasing or decreasing relative to gluconeogenesis by monitoring changes in relative flux through pathway E.

**TABLE I**

**RELATIVE FLUX OF CARBON-13 THROUGH PATHWAYS OF GLUCONEOGENESIS**

Relative Flux (%)	Pathway		
	A+B	C+D	E
	12-15	62-67	20-21

Let us now return to the synthesis of glucose. The liver spectrum taken after 140 minutes of perfusion (see Fig. 8) shows detectable resonances from all the carbon positions in glucose. This labeling pattern indicates that, in contrast to glutamate, more than one metabolic pathway contributes to the formation of glucose. Figure 11 shows five possible pathways. (Other pathways

exist but yield very little glucose.) Note that two pairs of these pathways (A and B, C and D) are degenerate in the sense that they yield identically labeled forms of glucose.

What fraction did each pathway contribute to the total amount of synthesized glucose? Or equivalently, what relative amount of carbon-13 passed through each pathway? We can obtain this information

## Regulation of Gluconeogenesis by NADH/NAD<sup>+</sup> Ratios

It is relatively easy to probe the regulatory mechanisms of gluconeogenesis by adding other substrates to the perfusate and determining their effects on the relative fluxes through the pathways and on the accumulation of various intermediates. We have focused initially on substrates designed to alter the ratio of the reducing agent, NADH to the oxidizing agent NAD<sup>+</sup>. As mentioned earlier, these coenzymes participate in many of the key reactions of metabolism and the NADH/NAD<sup>+</sup> ratio is believed to have an important regulatory effect on metabolism. This ratio changes with variations in oxygen supply and substrate availability.

What happens to the relative fluxes through the pathways when NADH levels are raised in the mitochondria alone, in the cytosol alone, or in both? How, under these various conditions, does the liver dispose of the amino groups lost by alanine? What happens to Krebs cycle activity? Might any of the observed effects be used as clinical markers of disorder? To determine the effects of altered NADH/NAD<sup>+</sup> ratios, we monitored gluconeogenesis from labeled alanine in perfused livers before and after adding, separately, the following substrates to the perfusate:

- 3-hydroxybutyrate, which produces NADH only in the mitochondria through action of the mitochondrial enzyme  $\beta$ -hydroxybutyrate dehydrogenase;
- ethanol, which produces NADH first in the cytosol through the reaction  $\text{ethanol} + \text{NAD}^+ \xrightarrow{\text{cytosolic enzyme}} \text{acetaldehyde} + \text{NADH}$  and then in the mitochondria through the reaction  $\text{acetaldehyde} + \text{NAD}^+ \xrightarrow{\text{mitochondrial enzyme}} \text{acetate} + \text{NADH}$ ;

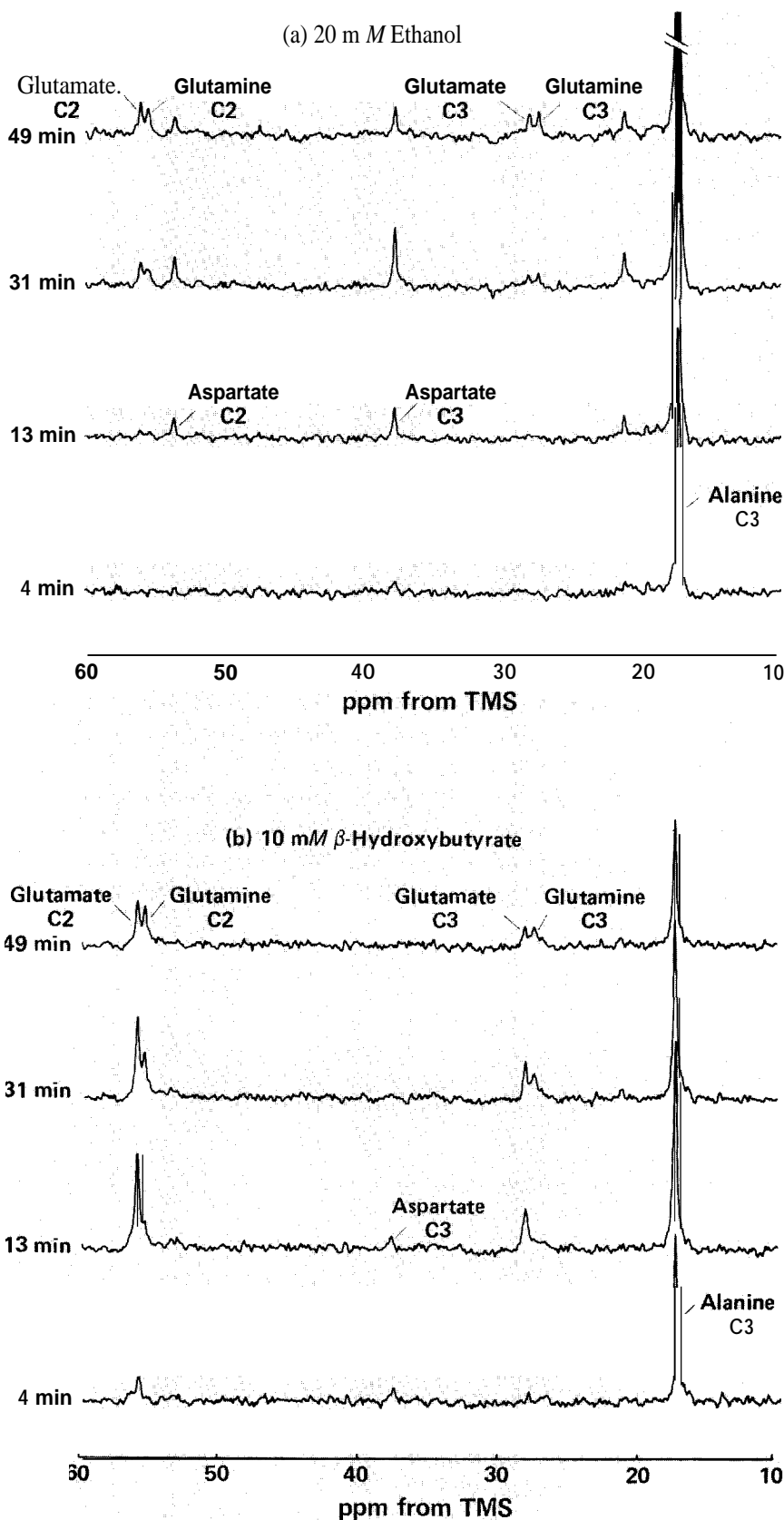


Fig. 13. Carbon-13 difference spectra of perfused liver during gluconeogenesis from 8-millimolar [<sup>3-<sup>13</sup>C</sup>]alanine in the presence of (a) 20-millimolar ethanol and (b) 10-millimolar  $\beta$ -hydroxybutyrate. Both these substances cause transient accumulation of aspartate, but the effect is much more pronounced in the case of ethanol.

**TABLE II****EFFECTS OF ETHANOL,  $\beta$ -HYDROXYBUTYRATE, AND REDUCED OXYGEN ON GLUCONEOGENESIS IN PERFUSED LIVER**

	Relative Carbon-13 Flux through Pathways (%)			Amino Acid Accumulated during First Hour
	A+%	C+D	E	
<b>Ethanol</b>				
Control	12	67	20	Glutamate
Ethanol	5	83	11	Aspartate, then glutamate
Ethanol plus disulfiram	7	79	14	Glutamate
<b><math>\beta</math>-Hydroxybutyrate</b>				
Control <sup>a</sup>	20	60	20	Glutamate
$\beta$ -Hydroxybutyrate	11	62	25	Very little aspartate, then glutamate
<b>Reduced Oxygen</b>				
Control	15	62	21	Glutamate
One-ninth oxygen	21	66	12	Glutamate

<sup>a</sup>Calculation of the relative fluxes in this experiment was complicated by the appearance of some label at carbon 4 of glutamate.

- ethanol plus the drug disulfiram, which specifically inhibits the mitochondrial reaction above and therefore produces NADH only in the cytosol.

In addition, we also monitored gluconeogenesis from labeled alanine in a liver perfused with a medium containing one-ninth the usual supply of oxygen.

Table 11 summarizes the effects of these changed conditions on the relative fluxes of carbon-13 from alanine through the pathways of gluconeogenesis. The relative fluxes given in the table represent averages during each three-hour experiment. The table also indicates which amino acid intermediates accumulated during the first hour of each experiment.

**CHANGES IN RELATIVE FLUXES.** We do not have a definitive interpretation of all the data. In particular, the data for reduced oxygen supply is puzzling. As expected,

alanine utilization and glucose production are reduced markedly. However, the increase in flux through pathways A and B relative to pathways C and D has no simple explanation. The decrease in the relative flux through pathway E is even more surprising since this indicates that Krebs cycle activity is decreased more than gluconeogenesis. Since the Krebs cycle must produce the ATP needed for gluconeogenesis, where does the ATP come from? A plausible hypothesis is that when the oxygen supply is reduced, other processes requiring ATP slow down much more than gluconeogenesis so that ATP is available despite the reduced activity of the Krebs cycle. But this hypothesis needs further investigation.

Addition of ethanol to the perfusate also results in a lower relative flux through pathway E. Again this indicates a decrease in Krebs cycle activity relative to gluconeogenesis, but in this case the decrease is to be expected. Ethanol oxidation generates the NADH required for gluconeogenesis and for

ATP production and thus reduces the requirements for NADH production by the Krebs cycle. These data are consistent with our understanding that the primary function of the Krebs cycle during gluconeogenesis is to supply NADH rather than to provide a pathway for conversion of the alanine skeleton into glucose. Further, these data demonstrate that Krebs cycle activity during gluconeogenesis is regulated by the cell's requirements for ATP and NADH.

The other changes in the relative fluxes of label give additional information about the interrelationships between gluconeogenesis and the urea cycle and the role of various metabolites shuttles across the mitochondrial membrane. However, a full discussion of these related topics is well beyond the intended scope of this article.

**ACCUMULATION OF ASPARTATE.** An interesting phenomenon is the transient accumulation of large amounts of aspartate in the presence of ethanol (Fig. 13a). Only small amounts accumulated in the presence of  $\beta$ -hydroxybutyrate (Fig. 13b) and none was seen in the other experiments. We were particularly interested in understanding this result because accumulation of an intermediate like aspartate might turn out to be a significant clue that the liver is under stress.

As shown in Fig. 6, the amino acid aspartate is formed from the Krebs cycle intermediate oxaloacetate. Like malate, it provides a 4-carbon skeleton for gluconeogenesis. Aspartate accumulates during the first hour of perfusion, acting as a sink for alanine's amino group, and then gradually disappears. While aspartate is accumulating, almost all of the label from alanine is incorporated into aspartate, and very little synthesis of glucose is detected. Eventually, glutamine and urea serve as sinks for the amino group, the aspartate (and later, the glutamate) resonances decrease, and the label from alanine is incorporated into glucose.

Aspartate accumulates when NADH/

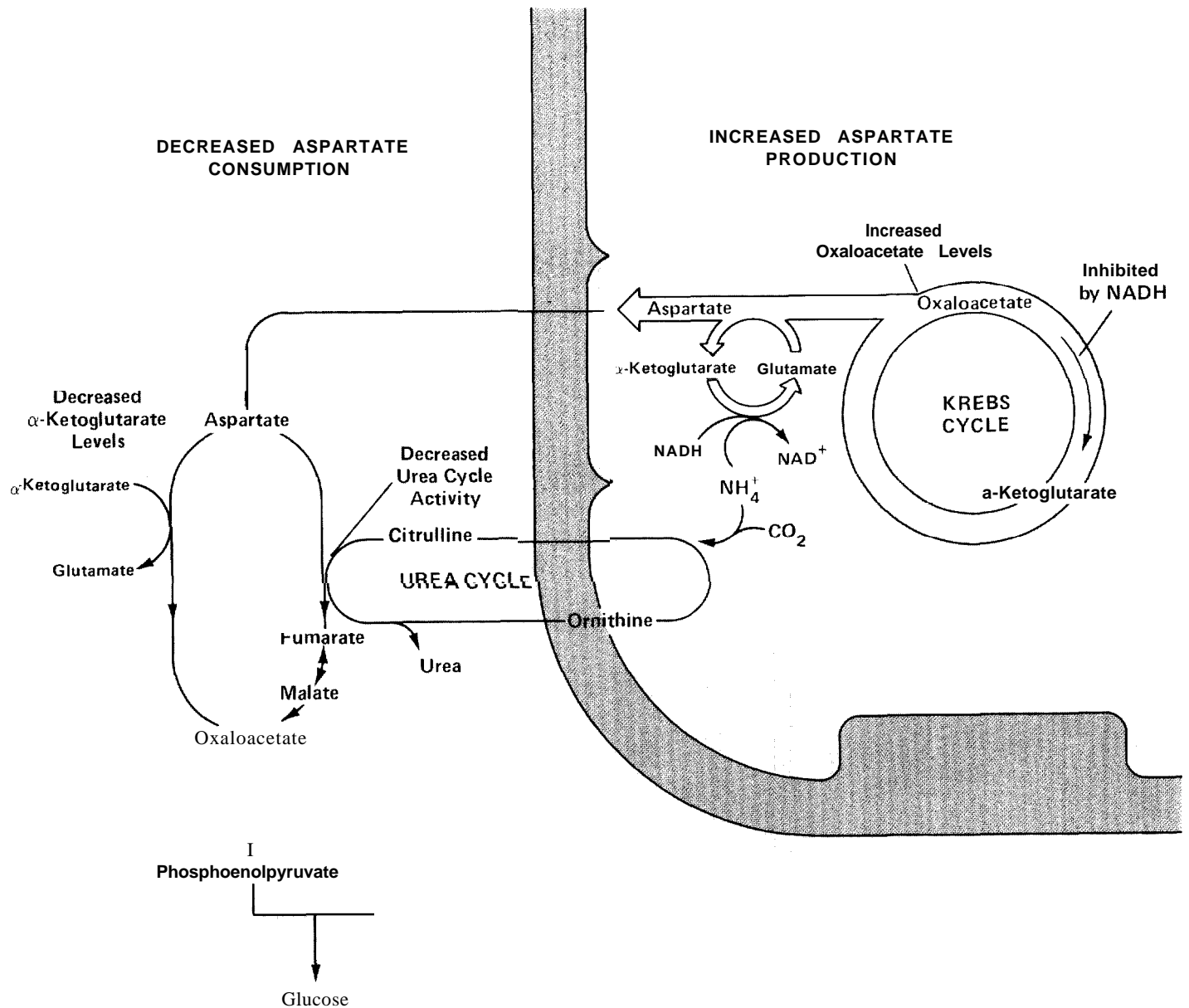
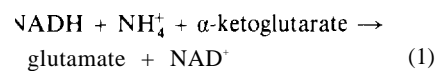


Fig. 14. Proposed mechanism for aspartate accumulation during gluconeogenesis from [3-<sup>13</sup>C]alanine in the presence of ethanol.

NAD<sup>+</sup> ratios are increased by ethanol in both the cytosol and the mitochondria. Why? We propose one possible mechanism, which is illustrated in Fig. 14. The accumulation of aspartate suggests that its rate of production in the mitochondria is increased relative to its rate of consumption in the cytosol. We suggest that the increased concentration of NADH in the mitochondria resulting from oxidation of ethanol is responsible not only for increased production of aspartate in the mitochondria but also for its decreased consumption in the cytosol.

Increased NADH/NAD<sup>+</sup> ratios affect the production of aspartate by altering the concentration of  $\alpha$ -ketoglutarate relative to that of oxaloacetate. (These two  $\alpha$ -keto acids serve as acceptors for alanine's amino group

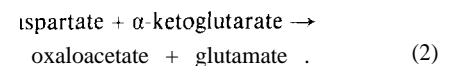
through a reaction known as transamination. Transamination of  $\alpha$ -ketoglutarate, a 5-carbon  $\alpha$ -keto acid, yields glutamate, whereas transamination of oxaloacetate, a 4-carbon  $\alpha$ -keto acid, yields aspartate.) A high NADH/NAD<sup>+</sup> ratio drives the reaction



far to the right and thus lowers the concentration of  $\alpha$ -ketoglutarate. In addition a high NADH/NAD<sup>+</sup> ratio inhibits several of the enzymes responsible for conversion of oxaloacetate to  $\alpha$ -ketoglutarate in the Krebs cycle. These two effects increase the concentration of oxaloacetate relative to that of  $\alpha$ -

ketoglutarate, and consequently oxaloacetate, rather than  $\alpha$ -ketoglutarate, serves as the acceptor for alanine's amino group.

After the aspartate has crossed the mitochondrial membrane to the cytosol, it is consumed by transamination to oxaloacetate or by reactions involving the urea cycle. The first of these pathways is the reaction



But the concentration of  $\alpha$ -ketoglutarate in the cytosol is not sufficient to promote reaction 2 because reaction 1 is occurring in the mitochondria. (Reaction 1 decreases the

concentration of  $\alpha$ -ketoglutarate in the mitochondria, and since  $\alpha$ -ketoglutarate can cross the mitochondrial membrane, its concentration in the cytosol is also decreased.) Thus increased NADH/NAD<sup>+</sup> ratios in the mitochondria inhibit the first pathway for aspartate consumption. We also suspect that the other pathway, which involves the urea cycle, may be inhibited by increased NADH/NAD<sup>+</sup> ratios in the cytosol.

We emphasize that in arriving at this mechanism for aspartate accumulation in the presence of ethanol we considered only a few of many interrelated processes and in particular neglected charge balance across the mitochondrial membrane. Charge balance is maintained by countertransport of an anion when aspartate or malate is shuttled across the membrane.

Is the proposed mechanism for aspartate accumulation consistent with our results for 3-hydroxybutyrate? This substrate, which increases the NADH/NAD<sup>+</sup> ratio only in the mitochondria, caused only a small accumulation of aspartate. We suggest that high NADH/NAD<sup>+</sup> ratios in the mitochondria relative to the cytosol tend to activate the transport of NADH from the mitochondria to the cytosol via the malate shuttle. This transport lowers the NADH/NAD<sup>+</sup> ratio in the mitochondria, and little aspartate accumulates. In this case the ammonium ion concentration is controlled by glutamate and glutamine production as it is for gluconeogenesis from alanine alone.

The data we have obtained are an insufficient basis for firm conclusions about the regulation of metabolism. They do, however, suggest a number of interesting hypotheses and questions. For example, the transient incorporation of label from alanine into the amino acids glutamate, aspartate, and (somewhat later) glutamine rather than into glucose indicates that the perfused liver, when first presented with alanine as a substrate for gluconeogenesis, uses not the urea cycle but the Krebs cycle intermediates  $\alpha$ -ketoglutarate and (in the presence of

ethanol) oxaloacetate as acceptors for the amino group derived from alanine. The continued depletion of Krebs cycle intermediates is bothersome in light of continued energy production by the Krebs cycle. Oxaloacetate in particular occupies a central role in the Krebs cycle, and accumulation of aspartate in the presence of ethanol may markedly alter already low (less than 0.2 millimolar) oxaloacetate concentrations.

Conventional bioanalytical techniques have revealed accumulation of glutamate, glutamine, and, in the presence of ethanol, aspartate in liver cells during gluconeogenesis from alanine. These conventional measurements were time-averaged, sometimes over periods as long as 90 to 100 minutes, and they suggested that the amino acid accumulation is a steady-state phenomenon. Our carbon-13 NMR measurements on perfused hamster livers, and those of other workers on rat liver cells and perfused mouse livers, permit almost real-time observation of changing metabolite concentrations and show that amino acid accumulation is transient. After an initial period the liver adapts to a new steady state in which its supply of 4-carbon skeletons required in the Krebs cycle is brought under control and amino groups are disposed of in the urea cycle.

How does the liver accomplish this? Does it depend on decreasing the NADH/NAD<sup>+</sup> ratio to a critical level? Or on adjusting the levels and activities of the appropriate enzymes to stimulate the urea cycle and modulate gluconeogenesis and the Krebs cycle? We don't know. Will these adjustments be impaired in the case of liver disease? Again, we don't know but strongly suspect that they will. To answer these and other questions about metabolism in the liver, baseline studies must be extended to other substrates for gluconeogenesis, especially pyruvate and lactate, in the presence or absence of other substrates that affect regulation, including ammonium ion, aspartate, glutamate, glutamine, fatty acids,

and ethanol.

The role of oxygen uptake by the liver will also have to be studied carefully under a variety of conditions. In the experiments we have performed thus far, we drastically reduced the supply of oxygen to the liver (one-ninth the normal amount) and, as expected, caused drastic reductions in the rates of gluconeogenesis and glutamate and aspartate production. To completely unravel the effect of oxygen, we must monitor metabolism as the oxygen supply is gradually reduced.

Metabolism in the liver is especially complex because of the many interdependent metabolic pathways. (Two important ones we have partially neglected here are lipid synthesis and degradation.) We have work under way, in collaboration with David E. Hoekenga of the University of New Mexico School of Medicine and the Albuquerque Veterans Administration Medical Center, on another vital but metabolically much simpler organ—the heart. In this organ oxygen supply to the tissue is of overriding importance because almost all (more than 90 percent) of its energy requirements are met through production of ATP by the electron transport chain, and the operation of this chain, in turn, is crucially dependent upon oxygen supply. Our work on the heart is currently focused on substrates thought to be involved in heart metabolism under anoxic conditions, such as glucose and amino acids. In addition, we plan to study the role of carnitine in heart metabolism. This molecule is a central control point in heart metabolism since it must link to fatty acids before they can enter the mitochondria and be oxidized. Carnitine has also been used to protect the heart against ischemic injury, but the mechanism through which this protection is conferred is uncertain. Clifford J. Unkefer of our group has recently devised a method for synthesizing <sup>13</sup>C-labeled carnitine, and we expect to learn a great deal about its functions during anoxia and ischemia from carbon-13 NMR studies on perfused hearts.

## Future Prospects

Baseline carbon-13 NMR studies of the type described here are being carried out in several laboratories. Raymond L. Nunnally of the University of Texas Health Science Center in Dallas is studying metabolism in perfused hearts and in the hearts of live rabbits and dogs with the intent of using NMR to define the extent and location of myocardial infarctions, to assess the temporal evolution of irreversible tissue damage, and to monitor the course of drug therapy. Similarly, Robert G. Shulman of Yale University, Sheila M. Cohen of the Merck Institute of Therapeutic Research, and John R. Williamson of the University of Pennsylvania are carrying out baseline metabolic studies on perfused livers and hearts and on livers, hearts, and brains of live animals. In another Los Alamos study Laurel O. Sillerud is studying metabolism in adipose tissue as a prelude to studying insulin resistance in diabetes and fat-trapping lesions in chronic obesity. Concurrently, a great deal of progress has been made in applying phosphorus-31 NMR to studies of ATP production and utilization. (Since phosphorus-31 is a naturally abundant isotope, these studies do not require labeling techniques.) Phosphorus-31 NMR is in fact already being used in clinical applications.

The ultimate objective of our research, and that of others in the field, is the study, diagnosis, and treatment of disease. Realizing this objective requires the pursuit of a number of projects, including the following:

- extend the baseline NMR studies on perfused organs and animals;
- develop efficient, large-scale processes for synthesis of selectively labeled compounds;
- design and construct magnets and radio-frequency coils with improved sensitivity and volume resolution;
- assess more completely the biological effects of magnetic fields;

- develop close cooperation among NMR spectroscopists, physiologists, biochemists, and physicians; and
- extend the studies to human controls and to patients with clinically well-defined diseases.

As this article indicates, the first two projects are well under way, and we can expect their acceleration soon as more investigators enter the field. With regard to the third, we point out that the most severe limitation of NMR spectroscopy in general, and carbon-13 NMR spectroscopy especially, is its relatively low sensitivity. The magnet and radio-frequency technology available at present limit real-time kinetic studies of metabolism in NMR to small, soluble metabolites (like glucose and alanine) present at concentrations exceeding 0.5 millimolar (500 micromolar). By way of comparison, recently developed electrochemical methods based on microelectrodes inserted into living cells can detect certain metabolites at concentrations as low as about 0.1 micromolar. The sensitivity of NMR experiments can be increased to some degree by sacrificing time resolution, that is, by averaging the signal over longer periods. However, for many metabolic studies the loss in time resolution is unacceptable. Advances in the design of more sensitive radio-frequency coils offer the most promise for increasing the sensitivity of *in vivo* NMR measurements, perhaps by a factor of ten. To this end Eiichi Fukushima of Los Alamos and Stephen B. W. Roeder of San Diego State University have designed and constructed novel radio-frequency coils. They have also begun to design magnets that provide the high, homogeneous magnetic fields required for human studies but do not confine the subject as do conventional magnets. We would welcome industry's involvement in this project, since the supply of NMR equipment—especially appropriate, reliable superconducting magnets—will probably be the major bottleneck in the development of a

national program for NMR in medicine.

A key issue in the use of NMR in human studies is whether static and oscillating radio-frequency magnetic fields are safe. Many years of experience with particle accelerators and with NMR instruments have produced no firm evidence of any biological hazard from static magnetic fields. However, anecdotal evidence is not very satisfactory. It could, for example, unfairly implicate static magnetic fields as an amplifying factor in the highly individualistic behavior of high-energy physicists and NMR spectroscopists when, in fact, it might be a neutral or moderating one! A review of the studies performed to date indicates that fields less than 2 tesla do not produce harmful cellular, biochemical, or genetic effects in humans. Continued study in this area is necessary because we will need static field strengths greater than 2 tesla to achieve higher sensitivity. At some field strength we expect biological effects to be observable. For example, a 20-tesla magnetic field should reduce the velocity at which nerves conduct signals.

The hazards associated with radio-frequency magnetic fields are more complex, but the principal hazard is radio-frequency heating of tissue. This should not be a major concern at the low frequencies we use, especially in light of the short duration of the radio-frequency pulses. Further, the new probe designs of Fukushima and Roeder may reduce this hazard by minimizing dielectric and ohmic heating effects.

The last two projects are closely related. Until now the rate of development in this field has been controlled largely by NMR spectroscopists who either learned cell culture and organ perfusion techniques themselves or who developed associations with cell biologists and physiologists on an as-needed basis. As we move from cells and perfused organs to animals and humans, the quality and rate of development of NMR spectroscopy in medicine will be determined by the strength of interdisciplinary teams that can not only obtain and interpret the

NMR data but also provide clinical, biochemical, and physiological expertise. The New Mexico state legislature recently provided funds for an NMR Center at the University of New Mexico School of Medicine. This center, which NMR spec-

troscopists and biochemists from Los Alamos are helping to develop, will be a unique national facility with respect to the breadth and depth of the interdisciplinary team that will be applying NMR to animals and humans. ■

---

### Further Reading

N. A. Matwiyoff, R. E. London, and J. Y. Hutson, "The Study of the Metabolism of  $^{13}\text{C}$  Labeled Substrates by  $^{13}\text{C}$  NMR Spectroscopy of Intact Cells, Tissues, and Organs," in *NMR Spectroscopy: New Methods and Applications*, George C. Levy, editor (American Chemical Society, Washington, D. C., 1982), pp. 157-186.

R. G. Shulman, "NMR Spectroscopy of Living Cells," *Scientific American* Vol. 248, No. 1,86-93 (1983).

R. E. Gordon, P. E. Hanley, and D. Shaw, "Topical Magnetic Resonance," *Progress in NMR Spectroscopy* 15, 1-47 (1982).

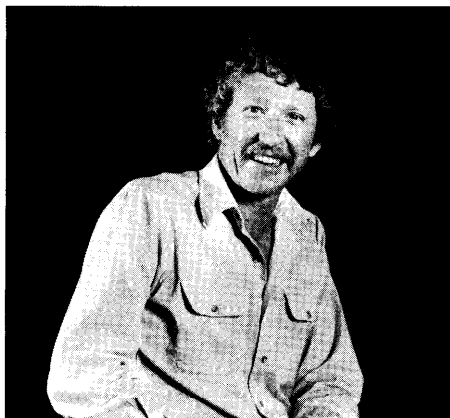
Robert E. London, "Intramolecular Dynamics of Proteins and Peptides as Monitored by Nuclear Magnetic Relaxation Measurements," in *Magnetic Resonance in Biology*, Jack S. Cohen, editor (John Wiley & Sons, New York, 1980), pp. 1-69.

Eiichi Fukushima and Stephen B. W. Roeder, *Experimental Pulse NMR: A Nuts and Bolts Approach* (Addison-Wesley Publishing Company, Inc., Reading, Massachusetts, 1981).

---

## AUTHORS

---



James R. Brainard received his B.A. from Hope College in Holland, Michigan and his Ph.D. in chemistry from Indiana University. He spent two years as a National Institutes of Health postdoctoral fellow at Baylor College of Medicine investigating the structure of plasma lipoproteins using nuclear magnetic resonance methods. Since coming to the Laboratory in December 1981, his research interests have focused primarily on the application of NMR and stable isotopes to the study of metabolism in perfused organs. A former avid sailor, Jim is still waiting for the reservoir behind Cochiti Dam to fill up.

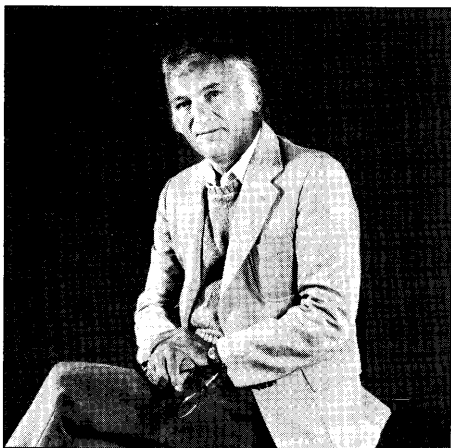
## AUTHORS



Judith Y. Hutson. I received a B.A. (1958) and an M.A. (1961) in chemistry and a Ph.D. (1968) in biochemistry from the University of Colorado. From 1961 to 1963 I did research at the Massachusetts Institute of Technology on the "early enzymes" of T-even bacteriophage infection in *E. coli*. In the fall of 1967 I came to Los Alamos with my husband and one small child. The first winter here was spent writing my Ph.D. thesis. By the summer of 1968, the degree was finished and we had a second child. A few months later I began research at the Laboratory on mammalian cells, on teratology, and on microbial biosynthesis with stable isotopes. For the past two years I have been involved with the research discussed in this article.

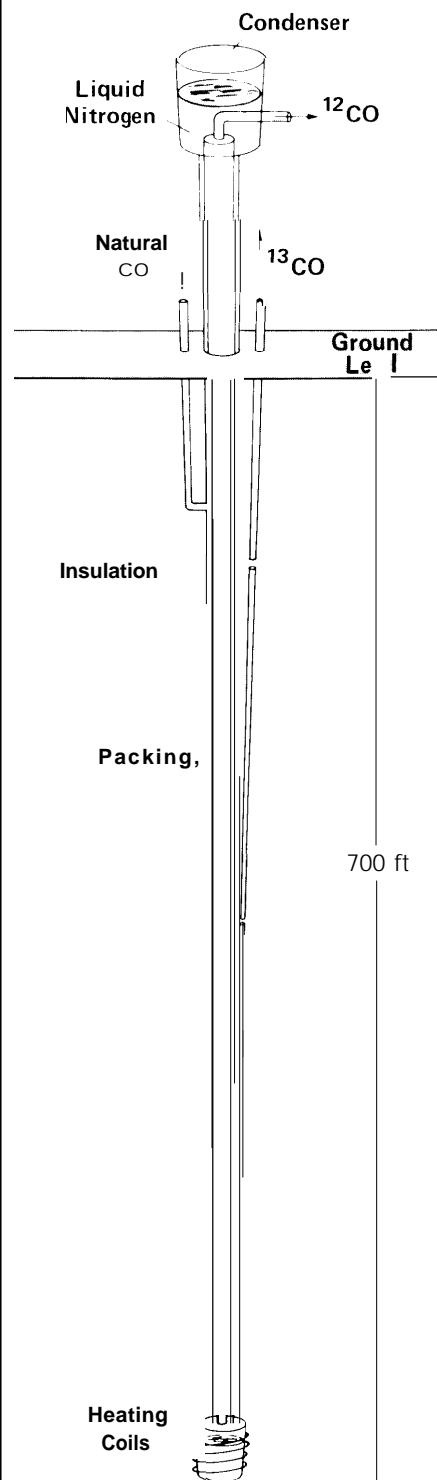


Robert E. London, a native of Brooklyn, New York, obtained his graduate degrees in physics and biophysical chemistry from the University of Illinois. He joined the Laboratory in 1973 as a postdoctoral fellow sponsored jointly by the Theoretical and Chemistry-Nuclear Chemistry divisions and in 1975 became a staff member in the Inorganic and Structural Chemistry Group. He has an interest in both theoretical and experimental aspects of the study of biological systems using nuclear magnetic resonance methods and has authored or coauthored approximately sixty-five papers in this field. A dedicated and hard working scientist, London worked at the Laboratory for three years before noticing that it was situated in the mountains of New Mexico.



Nicholas A. Matwyoff was born in Ann Arbor and raised in northern Michigan. He received his B.S. in chemistry from the Michigan College of Mining and Technology in 1959 and his Ph.D. in chemistry from the University of Illinois in 1963. Following a year as a National Science Foundation postdoctoral fellow at Stanford University, he joined the chemistry faculty at Pennsylvania State University. He moved to the Laboratory in 1968 to start an NMR project associated with a program on fluorine and actinide chemistry. As the stable isotope program at the Laboratory developed, his interests in NMR evolved to the study of biological systems labeled with carbon-13. He led the National Stable Isotopes Resource from its establishment in 1974 until 1982. At present he is Deputy Leader of the Isotope and Nuclear Chemistry Division.

## RELATED WORK



# Stable Isotope Production

## — a distillation process

by Nicholas A. Matwiyoff, Berthus B. McInteer, and Thomas R. Mills

**A** 700-foot distillation column is far from ordinary, but the Laboratory was forced to this length to separate the rare but stable isotope carbon-13 from the common isotope carbon-12 by distillation of carbon monoxide. In somewhat shorter distillation columns the Laboratory also enriches the even rarer stable isotopes nitrogen-15, oxygen-17, and oxygen-18. Produced in the western hemisphere only at Los Alamos, these enriched stable isotopes are used as tracers in many research areas ranging from metabolism to agriculture to atmospheric circulation.

Distillation, one of the oldest and most

*Schematic drawing of the Los Alamos distillation column for separating the naturally occurring mixture of  $^{12}\text{C}0$  and  $^{13}\text{C}0$ . The 700-foot column is supported over most of its length within a hole in the ground. The packing (spherical or saddle-shaped pieces of ceramic or metal provides surface area for contact between liquid and vapor phases. The column is cooled initially to liquid nitrogen temperature as natural carbon monoxide enters, rises to the condenser, and liquefies. The liquid flows downward and cools the column as it vaporizes. When liquid carbon monoxide collects at the bottom, it is vaporized by carefully regulated heat. At equilibrium a downflow of liquid repeatedly contacts upstreaming vapor, and the more volatile component accumulates at the condenser.*

effective methods for separating mixtures, exploits differences in the boiling points of the components. Two familiar examples of its beneficial applications are the separation of hydrocarbons from crude oil and the production of a beverage with a high alcohol content and a distinctive flavor from sour mash.

Distillation is most often applied to mixtures whose components have boiling points that are above 50 degrees Celsius and that differ from one another by more than 10 degrees. Separation of such mixtures can then be carried out in relatively short (10- to 30-foot) columns. In contrast, the boiling points of the various isotopic forms of carbon monoxide or nitric oxide are very low [only slightly higher than the boiling point (-196 degrees Celsius) of liquid nitrogen] and, more important, differ by only tenths of a degree. Small as these differences may be, they are larger than those exhibited by most other compounds of carbon, oxygen, and nitrogen.

The boiling points of  $^{12}\text{C}0$  and  $^{13}\text{C}0$  differ by less than 0.1 degree Celsius (more precisely, their vapor pressures differ by less than 0.8 percent). To separate the two, the Laboratory built a 700-foot distillation column—probably the longest in existence. This engineering marvel, developed by B. B. McInteer, T. R. Mills, and J. G. Montoya, produces 20 kilograms per year of 99+ atomic percent carbon-13. The problem of supporting such a long column was solved economically by lowering it into a cased, 15-inch-diameter hole in the ground, but this method of support prevents access for repair. Design and construction of the system there-

fore required the greatest care. The length changes (about 2 feet) that occurred when the system was initially cooled to the temperature of liquid nitrogen for operation (or that will occur should shutdown be necessary) demanded particular accommodation. The welds joining the thirty-five 20-foot sections were thoroughly tested for soundness, and the gas feed lines were fitted with expansion joints. Proof that the system met the highest standards of design and construction is its continuous operation without incident since 1978.

Since the vapor pressures of the various isotopic forms of nitric oxide differ more from each other (2.7 percent in the case of  $^{14}\text{N}^{16}\text{O}$  versus  $^{15}\text{N}^{16}\text{O}$ ) than do those of carbon monoxide, the two distillation columns at Los Alamos for separating them are "only" 150 and 270 feet long. These systems are complicated, however, by the large number of product streams ( $^{14}\text{N}^{16}\text{O}$ ,  $^{14}\text{N}^{17}\text{O}$ ,  $^{14}\text{N}^{18}\text{O}$ ,  $^{15}\text{N}^{16}\text{O}$ ,  $^{15}\text{N}^{17}\text{O}$ , and  $^{15}\text{N}^{18}\text{O}$ ) and by the necessity, since liquid nitric oxide is a high explosive, for barricades and remote controls. Nonetheless the two columns have been operated routinely since 1975 with an annual production capacity of 18 to 20 kilograms of nitrogen-15 at enrichments of up to 98 percent and 1 kilogram of oxygen-17 and 13 kilograms of oxygen-18 at enrichment of better than 40 and 95 atomic percent, respectively.

Under the guidance of McInteer and Mills, research has been directed recently to development of distillation methods for separating stable isotopes of heavier elements that are used as targets in the production of short-lived radioisotopes for nuclear medicine. ■

# Synthesizing Labeled Compounds

by Robert E. London, Nicholas A. Matwiyoff, Clifford J. Unkefer, and Thomas E. Walker

## RELATED WORK

Among the applications for the Laboratory's harvest of carbon monoxide enriched in carbon-13 are metabolic studies based on NMR spectroscopy. But first the isotope and its nuclear magnetic moment label must be incorporated at chosen sites in biochemical substances such as sugars and amino acids. The Laboratory has pioneered in developing chemical and biochemical methods for accomplishing this often intricate task.

For example, T. W. Whaley and R. M. Blazer of Los Alamos and Robert Barker and coworkers of Cornell University devised a chemical process (Fig. 1) for preparing a labeled form of the most common sugar, D-glucose. The essential reactant is  $^{13}\text{C}$ -labeled hydrogen cyanide ( $\text{H}^{13}\text{CN}$ ), which is obtained from  $^{13}\text{C}$ -enriched carbon monoxide by the reactions  $^{13}\text{CO} + \text{H}_2 \xrightarrow{\text{Ni}} ^{13}\text{CH}_4$  and  $^{13}\text{CH}_4 + \text{NH}_3 \xrightarrow{\text{Pt}} \text{H}^{13}\text{CN}$ . The labeled hydrogen cyanide is then reacted with the 5-carbon sugar D-arabinose to form a mixture of D-[1- $^{13}\text{C}$ ]glucononitrile and D-[1- $^{13}\text{C}$ ]mannononitrile, which is then converted to a mixture of D-[1- $^{13}\text{C}$ ]glucose and D-[1- $^{13}\text{C}$ ]mannose.

Since D-mannose is of limited utility and yet forms the bulk (75 percent) of the product, considerable effort has been directed to investigating various means for catalyzing its conversion to D-glucose, Barker and coworkers found recently that molybdate ion ( $\text{MoO}_4^{2-}$ ) is an effective catalyst, but NMR studies showed unequivocally that this catalyst converts D-[1- $^{13}\text{C}$ ]mannose to D-[1- $^{13}\text{C}$ ]glucose rather than the expected D-[1- $^{13}\text{C}$ ]glucose. This result is but one example of the unique insights into the course of chemical reactions provided by isotopic labeling and NMR spectroscopy.

Chemical syntheses such as the Barker process are sometimes the only practical route to a particular labeled compound but are often beset by difficulties: many are multi-step and hence lengthy, labor-intensive, and costly, and the yield of the labeled

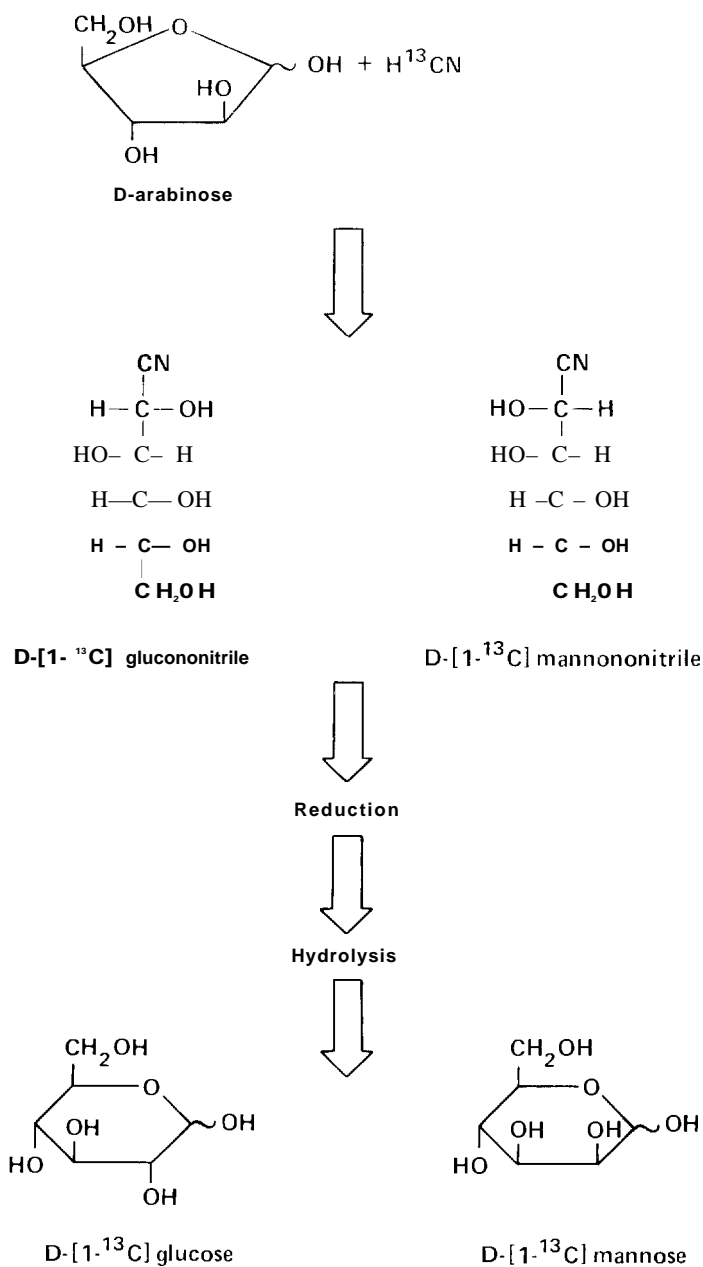
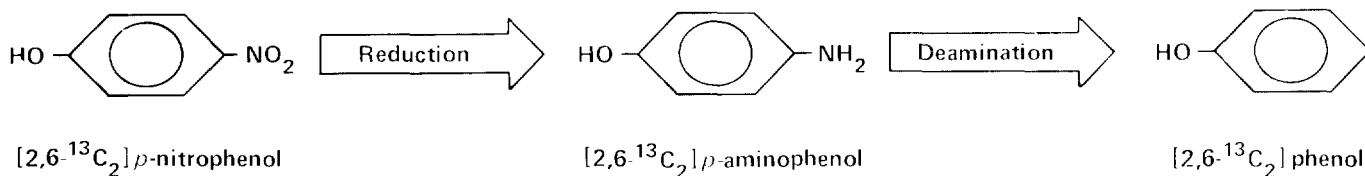
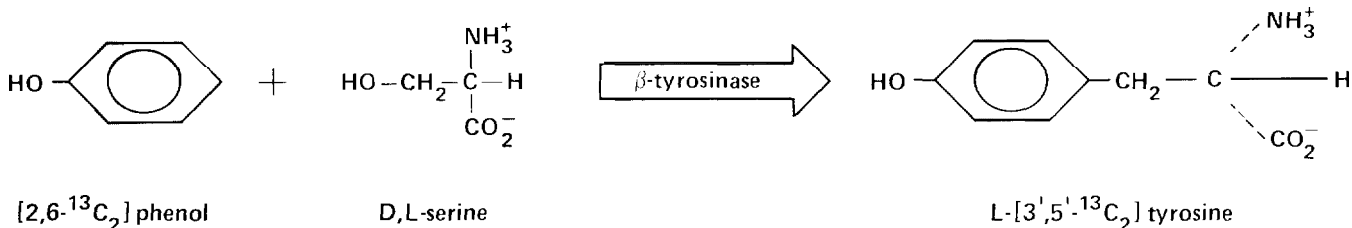


Fig. 1. Synthesis of  $^{13}\text{C}$ -labeled D-glucose, a 6-carbon sugar, involves adding a labeled nitrile group to the 5-carbon sugar D-arabinose by reaction with labeled hydrogen cyanide. The product of this reaction, a mixture of labeled nitriles of D-glucose and D-mannose (another 6-carbon sugar), is then reduced and hydrolyzed to a mixture of the labeled sugars. The two sugars are separated by absorption chromatography.

## CHEMICAL STEPS



## BIOCHEMICAL STEP



**Fig. 2.** Synthesis of  $^{13}\text{C}$ -labeled L-tyrosine, an amino acid, is accomplished in only three steps. The third and simplifying step, the reaction between labeled phenol and the amino acid serine, capitalizes on the ability of the bacterium *Erwinia*

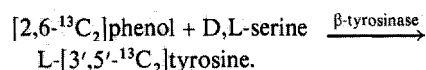
*herbicola* to produce large quantities of the necessary enzyme catalyst. Note that the reaction yields L-serine irrespective of whether the enzyme acts on D-serine, L-serine, or a mixture of the two isomers.

product may be disappointingly low because of diversion of the isotope into undesired products or positions. Since biochemical syntheses are often less subject to these difficulties, they are being pursued at Los Alamos—and with noteworthy success.

To illustrate, consider the synthesis of a labeled form of the amino acid L-tyrosine, which is present in nearly all proteins and is a precursor of the hormones epinephrine [adrenalin], norepinephrine, and thyroxine. V. J. Hruby of the University of Arizona has developed a ten-step chemical process for synthesizing a mixture of the D and L isomers of  $[3',5'\text{-}^{13}\text{C}_2]\text{tyrosine}$  from labeled *p*-nitrophenol. Based on the carbon-13 contained in the *p*-nitrophenol, the yield of the isomeric mixture is about 30 percent; separating the biologically active L isomer reduces the yield to 14 percent.

In contrast, T. E. Walker of Los Alamos and C. B. Storm of Howard University developed a combined chemical-biochemical method for preparing L- $[3',5'\text{-}^{13}\text{C}_2]\text{tyrosine}$  from the same labeled reactant in three steps with a yield of 80 percent. As in the synthesis of D-glucose, the labeled reactant, in this case *p*-nitrophenol, has its origins in  $^{13}\text{C}$ -enriched carbon monoxide:  $^{13}\text{CO} + \text{O}_2 \rightarrow ^{13}\text{CO}_2 \xrightarrow{\text{Cu,Cr,Zn}} ^{13}\text{CH}_3\text{OH}, ^{13}\text{CH}_2\text{OH} + \text{CO} \xrightarrow{\text{HI,Rh}} ^{13}\text{CH}_3\text{COOH}, ^{13}\text{CH}_2\text{COOH} + \text{Ba(OH)}_2 \rightarrow \text{Ba}(^{13}\text{CH}_2\text{COO})_2 \xrightarrow{\text{pyrolysis}} ^{13}\text{CH}_3\text{CO}^{13}\text{CH}_3 \xrightarrow{\text{condensation}} [2,6-^{13}\text{C}_2]p\text{-nitrophenol}$ . The tyrosine synthesis (Fig. 2) in-

volves two chemical steps that convert *p*-nitrophenol to phenol followed by a key biochemical step that converts phenol directly to L-tyrosine with the aid of the bacterium *Erwinia herbicola*. Under suitable conditions this microorganism manufactures high levels (up to 10 percent of its cell protein) of the enzyme  $\beta$ -tyrosinase. (This property was discovered in the course of Japanese research and development directed toward the use of microorganisms to produce large quantities of amino acids as food supplements.) After filling themselves with a surfeit of the enzyme, the bacteria are placed in a medium containing the labeled phenol and D-wine, L-serine, or a mixture of both, and the enzyme catalyzes the reaction



*E. herbicola's* generous supply of  $\beta$ -tyrosinase yields other labeled forms of L-tyrosine from variations on this reaction: L-[1-, 2-, or 3- $^{13}\text{C}$ ]tyrosine from unlabeled phenol and D, L-[1-, 2-, or 3- $^{13}\text{C}$ ]serine; and  $^{15}\text{N}$ -labeled L-tyrosine from unlabeled phenol unlabeled pyruvate, and  $^{14}\text{N}$ -labeled ammonia. (Nitrogen-15 is another isotope useful in metabolic studies based on NMR spectroscopy.)

Another example of biochemical synthesis is the use of the metabolically defective microorganism *Brevibacterium flavum* to

produce L-[2,4- $^{13}\text{C}_2$ ] glutamate in high yield from D-[1- $^{13}\text{C}$ ] glucose. The route to this amino acid (a salt of which, monosodium glutamate, is well known as the seasoning MSG) involves  $\alpha$ -ketoglutarate, one of the intermediates in the Krebs cycle. In normal organisms  $\alpha$ -ketoglutarate progresses through the Krebs cycle to succinate by action of the enzyme  $\alpha$ -ketoglutarate dehydrogenase. *B. flavum*, however, produces very little of the enzyme, and when these bacteria are grown in a medium containing glucose,  $\alpha$ -ketoglutarate accumulates and is converted, in the presence of ammonium ion, to L-glutamate. A sick but kindly organism, *B. flavum* suffers from the additional disorder of a leaky cell membrane, which allows passage of the glutamate into the medium where it can be recovered readily.

On the horizon for the biochemical synthesis program at Los Alamos is the use of recombinant DNA techniques to genetically engineer microorganisms with optimal properties for the production of labeled biochemical substances. By concurrently probing these microorganisms *in vivo* with NMR techniques, the metabolic consequences of the genetic engineering can be ascertained. This approach, being taken by C. J. Unkefer of Los Alamos in collaboration with J. K. Griffith of the University of New Mexico, may be one of the most significant research directions in stable isotope technology in this decade. ■

# Enzyme Structure and Interaction with Inhibitors

by Robert E. London

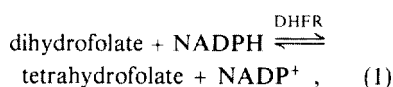
## RELATED WORK

The metabolic studies described in the previous article represent a relatively straightforward application of NMR spectroscopy. The positions of the various resonances and their heights allow one to determine the presence and amount of metabolic intermediates and products and, in turn, the specific metabolic pathways involved. These tracer studies with stable-isotope labels are thus directly analogous to studies with radiolabels such as carbon-14.

But NMR spectra contain a wealth of additional information. Changes in resonance position and shape under various conditions can reveal important structural and dynamic features of complex biological macromolecules. Here we will review some results of an extensive series of studies on the <sup>13</sup>C-labeled enzyme dihydrofolate reductase, or DHFR. The idea was to explore how much we could learn about structure and dynamics using NMR techniques in combination with isotopic labeling.

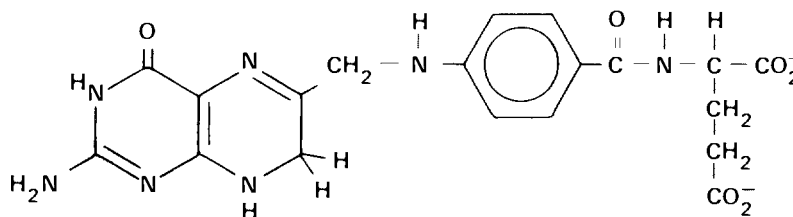
Enzymes are particularly interesting to study from this point of view since both their structure and dynamics may be important to their function of catalyzing biochemical reactions. In the familiar "lock and key" model of enzyme catalysis, a structurally rigid enzyme "lock" can bind only the structurally complementary substrate "keys." Extensive crystallographic data have also fostered this picture of enzymes as rigid structures. But recent evidence suggests that enzyme dynamics is also at work in recognition and catalysis.

We chose to study the enzyme DHFR because of its clinical relevance. Its function is to "activate" the vitamin folic acid by catalyzing the oxidation-reduction reaction



where dihydrofolate is an inactive form of folic acid, and tetrahydrofolate is its ac-

**Dihydrofolate**



**Methotrexate**

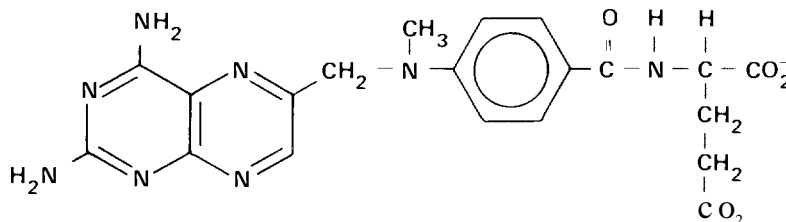


*Fig. 1. Substrate dihydrofolate and inhibitor methotrexate of the enzyme dihydrofolate reductase (DHFR). Note that the left most regions of the substrate and the inhibitor are similar in structure. Because these regions presumably interact strongly with the enzyme, they were labeled with carbon-13 (at the locations indicated by gray circles) for the purpose of studying enzyme/substrate and enzyme/inhibitor interactions.*

tivated form.\*

Tetrahydrofolate is required for the synthesis of thymidine, a component of DNA. Inhibiting the production of tetrahydrofolate therefore retards DNA synthesis and cellular growth. In fact, one treatment for the unregulated cellular replication that characterizes cancerous growth is to inhibit the production of tetrahydrofolate by administering drugs that bind with very high affinity to DHFR. These drugs, so-called antifolate inhibitors, are structurally quite similar to dihydrofolate (Fig. 1) and can bind at DHFR's "active site" far dihydrofolate, thereby preventing DHFR from catalyzing reaction 1. One goal of our studies was to understand, at the molecular level, why these

inhibitors have a very high affinity for DHFR. Such information can be of value for the design of even more potent and specific inhibitors of the enzyme.

DHFR is a medium-sized enzyme with a molecular weight of about 20,000, and its NMR spectrum in the absence of labeling would show only a low-intensity "background," due to naturally occurring carbon-13, of nearly 800 carbon resonances. Labeling specific portions of the enzyme with carbon-13 was therefore essential to

\*NADPH (nicotinamide adenine dinucleotide phosphate), a derivative of the vitamin niacin, is an enzyme cofactor involved in biological oxidation-reduction reactions.

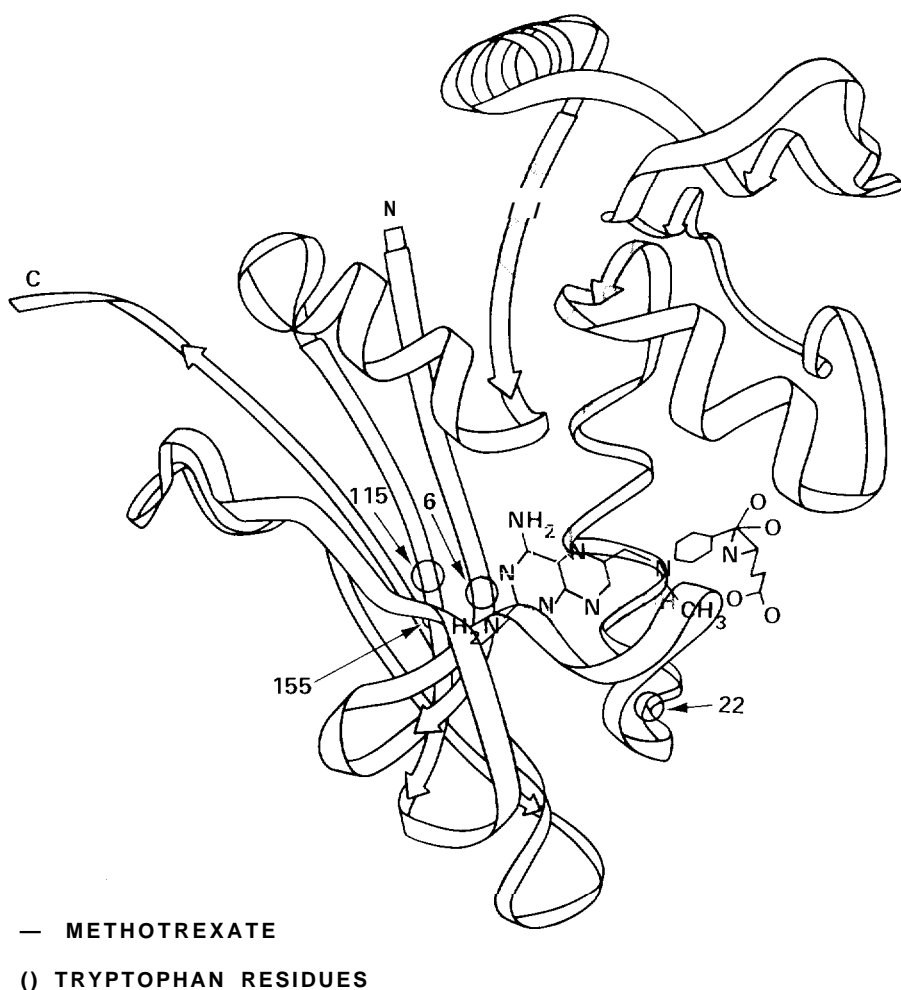


**Fig. 2.** Backbone ribbon drawing, showing the locations of the enzyme cofactor NADPH and of the inhibitor methotrexate, of the enzyme DHFR (a linked chain of 167 amino acid residues) derived from the microorganism *Lactobacillus casei*. [Adapted from J. T. Bolin, D. J. Filman, D.A. Matthews, R. C. Hamlin, and J. Kraut, *Journal of Biological Chemistry* 257, 13650 (1982).] By occupying the enzyme's active site for dihydrofolate, the inhibitor prevents DHFR from catalyzing the reaction that converts this inactive form of the vitamin folic acid to its active form. NMR spectra for DHFR derived from the microorganism *Streptococcus faecium* and containing the  $^{13}\text{C}$ -labeled residue of the amino acid tryptophan provided information about the dynamic of the enzyme and the interaction between enzyme and inhibitor. The approximate positions of the four tryptophan residues in DHFR derived from *S. faecium* and *L. casei* are those indicated in the drawing, if it is assumed that DHFR derived from *S. faecium* and *L. casei* are homologous.

enhance selected peaks and thereby reduce the complexity and increase the sensitivity of these studies.

X-ray crystallographic studies have shown that enzymes are long strings of peptide-linked amino acids (that is, the amino group of one acid residue binds to the carboxylic acid group of the next). These long strings of amino acids fold in a complex way to form a globular structure (Fig. 2). To study the sensitivity of NMR spectra to structure, we labeled selected amino acid residues of DHFR with carbon-13 and measured the spectra of the labeled enzyme in its globular form and again after its structure had been changed into a random coil by the addition of urea.

The carbon-13 labeling was accomplished by first labeling the amino acids methionine, arginine, and tryptophan and then growing the microorganism *Streptococcus faecium* in media containing one of these labeled amino acids. *S. faecium*, which is a good source of the enzyme DHFR, incorporates the labeled amino acids into the DHFR molecules. The labeled DHFR was then isolated from the microorganism, and its NMR spectra were obtained for the globular and random coil configurations. Figure 3 shows the results for DHFR labeled with  $[3-^{13}\text{C}]$ tryptophan. The spectrum for the globular form of DHFR shows several carbon-13 resonances corresponding to different positions along the polypeptide backbone and therefore to different chemical environments of the individual tryptophan residues within the enzyme. Note that most of these so-called chemical shifts disappear when the enzyme structure is disrupted into a random coil. Thus NMR spectra are sensitive to structure.

Looking more closely at the spectrum for the globular structure, we note that it has five resolved resonances although there are only four tryptophan residues in each enzyme molecule. Evidently a single tryptophan residue is responsible for the two adjacent peaks near 110 ppm. This splitting probably indicates that the enzyme takes on two dif-

## RELATED WORK

ferent configurations in the region of that particular residue.

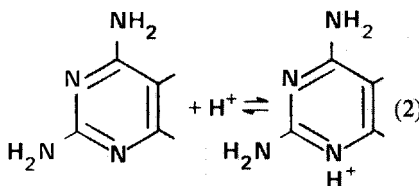
The resonance at 106 ppm is also noteworthy because it is much broader than the others, a fact suggesting that the residue responsible for the resonance is located in a portion of the enzyme that undergoes conformational changes with time. Spectra taken at different temperatures (Fig. 4) confirmed this suggestion. The resonance at 106 ppm (resonance 4) exhibits a strongly temperature-dependent linewidth believed to be associated with "breathing" of the enzyme. That is, the enzyme adopts an ensemble of molecular conformations leading to temperature-dependent dynamic behavior. Figure 4 also shows that this "breathing" phenomenon disappears when the enzyme is complexed with the inhibitor 3',5'-dichloromethotrexate. (The structure of this inhibitor is like that of methotrexate in Fig. 1 except that chlorine replaces hydrogen at positions 3 and 5 on the benzene ring.) The resonance then becomes sharp, indicating that a part of the binding energy between enzyme and inhibitor stabilizes a particular subset of enzyme conformations. For DHFR derived from *S. faecium* we found that the substrate dihydrofolate and each of the inhibitors studied lead to sharpening of resonance 4. In contrast, NADPH, the enzyme cofactor in reaction 1, does not significantly sharpen the resonance. Presumably, the NADPH binds to a portion of the enzyme molecule more remote from the particular tryptophan residue responsible for resonance 4.

The addition of substrate or inhibitor molecules can also lead to changes in resonance position, or chemical shifts. For example, the spectra at 15 degrees Celsius in Fig. 4 show that dichloromethotrexate causes a slight shift of resonance 1 to the right. Such chemical shifts reflect interactions between the enzyme and the bound molecules. In general, our results demonstrate the sensitivity of NMR spectra to the precise folded enzyme structure. Interactions among specific pairs of residues are important in produc-

ing chemical shifts, and these shifts are altered when the enzyme binds other molecules. Dynamic behavior such as "breathing" is also observable, but whether this behavior observed in DHFR is significant for catalysis (for example, whether it helps the enzyme to "recognize" the substrate dihydrofolate) is still an open question.

A second set of studies with DHFR was designed to investigate the basis for the high affinity between the inhibitor methotrexate and DHFR. Rather than labeling the enzyme, we chose to label the inhibitor. The label was placed in that portion of methotrexate thought to interact strongly with DHFR (see Fig. 1, where the position of the carbon-13 label is marked by a gray circle). We found that the NMR spectrum of a solution containing labeled methotrexate and DHFR exhibits two carbon-13 resonances, one corresponding to inhibitor molecules that are free in solution and one corresponding to inhibitor molecules that are tightly associated with the enzyme. The fact that the single carbon-13 label exhibits two resonances is a reflection of the very high affinity of methotrexate for the enzyme.

We then varied the pH of the solution containing the enzyme and the labeled inhibitor and found that the two resonances behave very differently (Fig. 5). The resonance ascribed to the uncomplexed inhibitor undergoes a large shift in position at a pH of about 5.7. This so-called titration behavior indicates that the uncomplexed inhibitor accepts a proton ( $H^+$ ) in the following reversible reaction:



The pH at which the curve's large shift is centered (5.7) is called the pK of this proc-

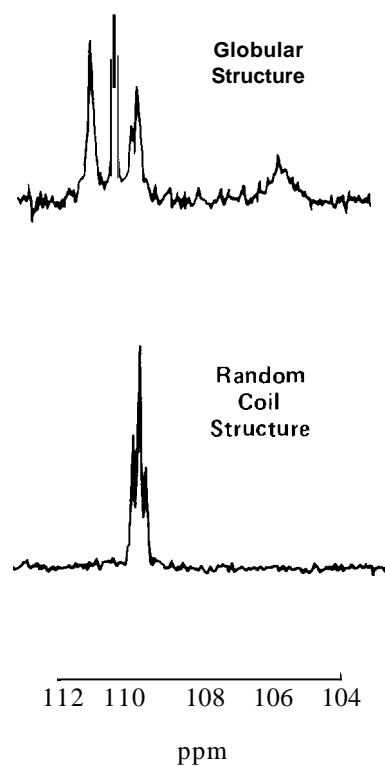
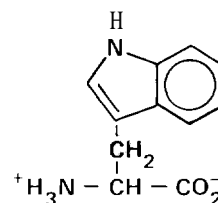


**Fig. 3. Carbon-13 NMR spectra for [3- $^{13}\text{C}$ ]tryptophan-labeled DHFR in its active globular form and in its random coil form. The structure of tryptophan is also shown, with the position of the carbon-13 label indicated by a gray circle. Note that the globular structure produces many more distinct resonances than does the random coil structure.**

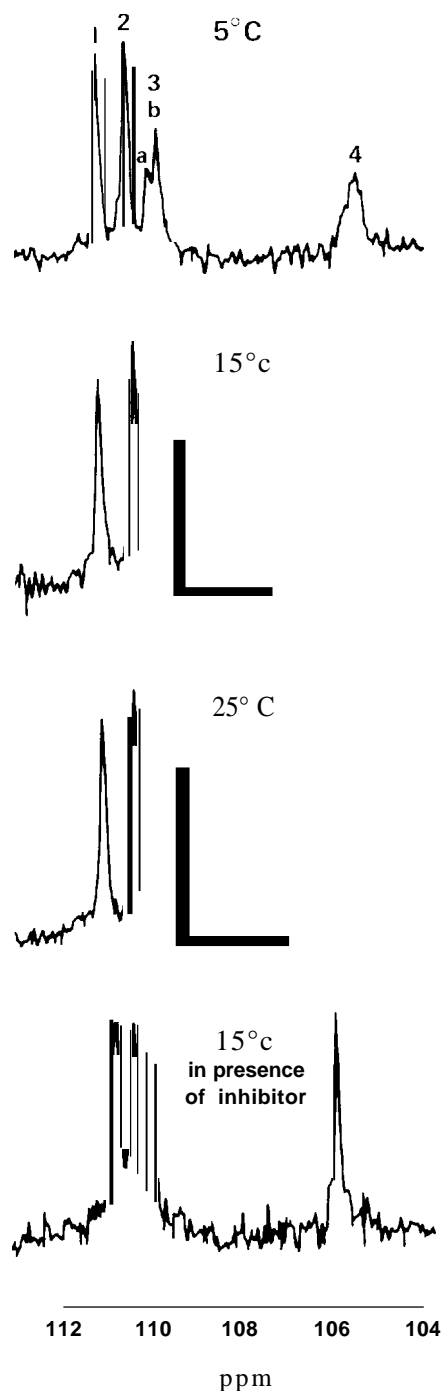


**Fig. 4.** Carbon-13 resonances observed for  $[3\text{-}^{13}\text{C}]$ tryptophan-labeled DHFR at various temperatures and at 15 degrees Celsius in the presence of the inhibitor 3',5'-dichloromethotrexate. Resonance 4 exhibits a temperature-dependent line-width that becomes a sharp resonance in the presence of the inhibitor. The tryptophan residue thought to be responsible for resonance 4 is labeled 6 in Fig. 2.

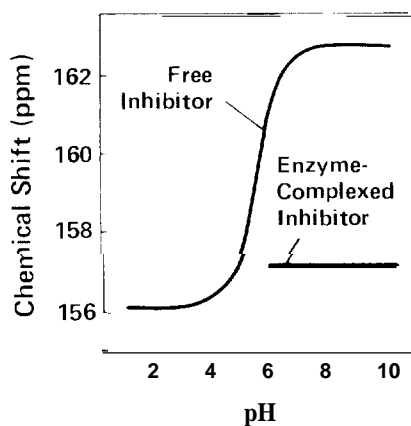


**Fig. 5.** Chemical shifts of the carbon-13 resonance for the inhibitor methotrexate (labeled as in Fig. 1) as a function of pH. When the enzyme DHFR is present (that is, at pH values above 5.5), two sets of resonances are observed, one corresponding to free methotrexate and one to the enzyme-complexed inhibitor. These results show that methotrexate in its protonated form has an extremely high affinity for the enzyme.

ess. It represents the pH value at which half of the molecules are protonated and half unprotonated. **Thus the one resonance observed for the uncompleted inhibitor is actually an average produced by its protonated and unprotonated forms.** In contrast, the resonance ascribed to the enzyme-complexed methotrexate remains fixed near the resonance of the protonated form of the uncompleted inhibitor. These data indicate that the protonated form of methotrexate is the potent enzyme inhibitor: in other words, a strong interaction between protonated methotrexate and the enzyme must be the critical factor in making methotrexate an effective inhibitor. This conclusion is supported by the x-ray crystallographic data of Matthews and coworkers at the University of California, San Diego. They found that in the crystalline state the enzyme-complexed methotrexate is protonated and hydrogen-bonded to a negatively charged amino acid (aspartate-26) of the enzyme.

Figure 5 shows that the pK for protonation of the enzyme-complexed inhibitor is well above 10, the highest pH value used in the study. Such a large difference between the pK of the enzyme-complexed inhibitor and that of the free inhibitor is a measure of the binding energy between the inhibitor and the enzyme. The strength of binding was not accurately known prior to these studies and had in fact been incorrectly determined using conventional ultraviolet spectroscopic techniques. It is an impressive achievement of the isotopic labeling/NMR method that of all the interactions among amino acid residues and between amino acids and solvent molecules that stabilize the enzyme structure, we can probe a single one and quantify its strength. ■

#### Acknowledgment

These studies were carried out at St. Jude's Research Hospital in Memphis, Tennessee in collaboration with Raymond L. Blakley, Lennie Cocco, and John Groff. Groff is currently on the staff of Abbott Laboratories.